remote sensing

MDPI

Article

Integrated Spatial Analysis of Forest Fire Susceptibility in the Indian Western Himalayas (IWH) Using Remote Sensing and GIS-Based Fuzzy AHP Approach

Pragya [1], Manish Kumar [1], Akash Tiwari [1], Syed Irtiza Majid [1], Sourav Bhadwal [1], Netrananda Sahu [2], Naresh Kumar Verma [3], Dinesh Kumar Tripathi [4] and Ram Avtar [5,*]

[1] Department of Geography, School of Basic Sciences, Central University of Haryana, Mahendragarh 123031, Haryana, India; pragyapalak2203@gmail.com (P.); manish.ks@cuh.ac.in (M.K.); akash200777@cuh.ac.in (A.T.); sirtiza212093@cuh.ac.in (S.I.M.); sourav200786@cuh.ac.in (S.B.)
[2] Department of Geography, Delhi School of Economics, University of Delhi, New Delhi, Delhi 110007, India; nsahu@geography.du.ac.in
[3] Special Centre for National Security Studies, Jawaharlal Nehru University, New Delhi, Delhi 110067, India; nkverma@mail.jnu.ac.in
[4] Rana Pratap Post Graduate College, Sultanpur 228001, Uttar Pradesh, India; tripathidk@rppgsultanpur.org
[5] Faculty of Environmental Earth Science, Hokkaido University, Sapporo 060-0810, Hokkaido, Japan
* Correspondence: ram@ees.hokudai.ac.jp

Abstract: Forest fires have significant impacts on economies, cultures, and ecologies worldwide. Developing predictive models for forest fire probability is crucial for preventing and managing these fires. Such models contribute to reducing losses and the frequency of forest fires by informing prevention efforts effectively. The objective of this study was to assess and map the forest fire susceptibility (FFS) in the Indian Western Himalayas (IWH) region by employing a GIS-based fuzzy analytic hierarchy process (Fuzzy-AHP) technique, and to evaluate the FFS based on forest type and at district level in the states of Jammu and Kashmir, Himachal Pradesh, and Uttarakhand. Seventeen potential indicators were chosen for the vulnerability assessment of the IWH region to forest fires. These indicators encompassed physiographic factors, meteorological factors, and anthropogenic factors that significantly affect the susceptibility to fire in the region. The significant factors in FFS mapping included FCR, temperature, and distance to settlement. An FFS zone map of the IWH region was generated and classified into five categories of very low, low, medium, high, and very high FFS. The analysis of FFS based on the forest type revealed that tropical moist deciduous forests have a significant vulnerability to forest fire, with 86.85% of its total area having very high FFS. At the district level, FFS was found to be high in sixteen districts and very high in seventeen districts, constituting 25.7% and 22.6% of the area of the IWH region. Particularly, Lahul and Spiti had 63.9% of their total area designated as having very low FSS, making it the district least vulnerable to forest fires, while Udham Singh Nagar had a high vulnerability with approximately 86% of its area classified as having very high FFS. ROC-AUC analysis, which provided an appreciable accuracy of 79.9%, was used to assess the validity of the FFS map produced in the present study. Incorporating the FFS map into sustainable development planning will assist in devising a holistic strategy that harmonizes environmental conservation, community safety, and economic advancement. This approach can empower decision makers and relevant stakeholders to take more proactive and informed actions, promoting resilience and enhancing long-term well-being.

Keywords: forest fire susceptibility; remote sensing; GIS-based Fuzzy-AHP; physiographic; meteorological; anthropogenic drivers; Indian Western Himalayas

check for updates

Citation: Pragya; Kumar, M.; Tiwari, A.; Majid, S.I.; Bhadwal, S.; Sahu, N.; Verma, N.K.; Tripathi, D.K.; Avtar, R. Integrated Spatial Analysis of Forest Fire Susceptibility in the Indian Western Himalayas (IWH) Using Remote Sensing and GIS-Based Fuzzy AHP Approach. *Remote Sens.* **2023**, *15*, 4701. https://doi.org/10.3390/rs15194701

Academic Editors: Nicola Casagli, Matteo Gentilucci and Gilberto Pambianchi

Received: 28 August 2023
Revised: 20 September 2023
Accepted: 21 September 2023
Published: 25 September 2023

Copyright: © 2023 by the authors. Licensee MDPI, Basel, Switzerland. This article is an open access article distributed under the terms and conditions of the Creative Commons Attribution (CC BY) license (https://creativecommons.org/licenses/by/4.0/).

1. Introduction

Forests are an essential natural resource that play a vital role in maintaining global ecological equilibrium and ensuring the long-term survival of human civilization [1–4].

A Food and Agriculture Organization (FAO) report suggests that the Earth's surface encompasses a total of 4.06 billion hectares (30.06%) of global forest coverage. Among these, ref. [5] estimated that approximately 420 million hectares of forested areas worldwide are subjected to annual burning, surpassing the entire land area of India. Besides deforestation, forest fires stand as one of the utmost significant threats to forest ecosystems on a global scale [6]. Forest fires are considered a catastrophic occurrence that has the potential to cause significant damage to forest ecosystems [7]. These fires represent a complex phenomenon that can stem from a combination of natural and human activities, under the influence of interrelated factors including fuel composition, weather conditions, geography, ignition sources, etc. [8]. According to [8], human activities are responsible for the predominant proportion of wildfire incidents (approximately 90%). In contrast, the remaining 10% of wildfires are triggered by natural lightning. Over the past several decades, there has been an increase in the number of forest fire incidents on a global scale, leading to heightened apprehension among the public and governmental bodies regarding the environmental and socioeconomic consequences of these fires [9].

Globally, Asia ranks as the fourth most affected continent, facing significant threats from forest fires [10]. Within the South Asian region, India emerges as the second most at-risk nation, with a 32% vulnerability rate, ref. [11]. Over the past two decades, India has witnessed a staggering tenfold increase (52%) in intense forest fire incidents [12]. These fires primarily impact the deciduous forests in central and southern India, as well as the forests within the western and eastern Himalayas [13–15]. Forest fires in India are widespread, encompassing a vast geographical area and arising from both natural and human factors. Each year, an estimated 3.73 million hectares of forest land experience burning, resulting in an approximate economic loss of about USD 110 million [16]. Forest fires in the Indian Western Himalayas (IWH) region are a persistent hazard that is further intensified by the changing climatic trends [17]. The IWH region is renowned for its rich biodiversity, pristine landscapes, and significant contribution to the provision of vital ecosystem services. The geographical area under consideration is characterized by diverse forest types, steep terrain, and a wide range of climatic conditions, making it particularly vulnerable to forest fires. The susceptibility of these forests to fire has been further exacerbated by climate-change-induced variations in temperature and precipitation patterns. States such as Uttarakhand, Himachal Pradesh, and Jammu and Kashmir are particularly vulnerable to forest fires due to the combined effects of climatic conditions, geographical features, vegetation types, and human activities [18]. The Indian Western Himalayas has witnessed significant forest fire incidents in recent decades, mainly concentrated during the hot and arid pre-monsoon season spanning from March to June [19,20]. Between 2001 and 2019, the burn area increased in Uttarakhand and Himachal Pradesh at a rate of 72.94 km^2 per year [21]. These fires not only pose a direct threat to forest ecosystems and wildlife but also have adverse impacts on air quality, water resources, and the livelihoods of local communities. Hence, as part of broader initiatives to tackle this challenge, effective fire management strategies, community engagement, the identification of forest fire vulnerability, and sustainable land management practices are crucial [22].

Through the utilization of geospatial techniques including remote sensing (RS), geographic information systems (GIS), and statistical methods, it becomes feasible to create a reliable spatial map outlining potential zones of forest fire risk across varying geographical regions. The adoption of geospatial methodologies empowers individuals to incorporate multiple models and processes, leading to precise outcomes within a concise timeframe. Since the 1970s, satellite-based remote sensing data have been used successfully to differentiate between areas affected by fire and those that are actively burning. This is achieved by measuring the temperature difference between the reflectance of vegetation and the reflectance of burned areas [23]. The identification and delineation of forest-fire-prone regions have emerged as crucial duties in modern times since they play a pivotal role in effectively controlling this calamity at a national level. Diverse categories of earth observation sensors, including multi- and hyper-spectral sensors, have already showcased their

precision within this field. Remote sensing satellite data using MODIS (moderate-resolution imaging spectroradiometer) play a pivotal role across multiple sectors, encompassing land cover classification, vegetation monitoring, climate analysis, and disaster management [24]. Its moderate geographical and temporal resolutions strike an optimal balance between detailed observations and comprehensive coverage, rendering it invaluable for analyses spanning from regional to global scales [25]. In the present study, the NDVI was extracted from MODIS Vegetation Indices-V6. Additionally, forest incident point data were acquired from MODIS/Visible Infrared Imaging Radiometer Suite (VIIRS), which was utilized to validate the FFS maps.

Over the past few decades, forest fires have received significant attention from researchers due to their devastating nature and their potential for causing substantial economic losses and ecological losses on a global scale. In recent times, the utilization of remote sensing (RS) and geographic information system (GIS) technologies has provided valuable insights for the field of forest fire susceptibility studies by integrating MCDM and ML techniques. The mapping of forest fire susceptibility involves the analysis of a multi-temporal dataset [26], and GIS tools play a crucial role in generating, managing, and integrating forest fire event databases alongside various causative factors. Numerous GIS-based forest fire susceptibility models have been employed in the literature, including the frequency ratio [27], random forest [28,29], artificial neural network [30], gradient boosting machine [31], support vector machine [29], and ensemble statistical machine learning models [32], which extensively employ geospatial data for analysis. These models have been widely adopted for the evaluation of susceptibility to various hazards based on the existing literature. While machine learning models are effective for making predictions in various fields, they present certain limitations when applied to macro-level studies because of the unavailability of sufficient training data [33]. MCDM, on the other hand, has emerged as a successful approach which provides a structured approach for dealing with complex problems involving multiple criteria and stakeholders, making it suitable for resolving macro-level complex decision making and policy analysis [34,35]. The analytical hierarchy process (AHP) was developed by [36] and is a prominent method within the field of MCDA. Using pairwise comparison matrices, this method is used to analyze the relative importance of various contributing factors and their related sub-categories. The technique may limit the decision maker's ability to appropriately express their preferred choice because of the probability of inconsistency in paired comparisons at a particular level [37–39]. In this study, the Fuzzy-AHP, developed by [40], was employed. The integration of AHP with fuzzy set theory was aimed at effectively addressing the challenges associated with MCDA. The Fuzzy-AHP employs the triangular fuzzy number (TFN) as a substitute for exact numerical values in order to get the final result. The utilization of TFNs has revealed significant advantages in assessing numerous factors that impact forest fires, as highlighted in several research studies [41–43]. Many researchers have used Fuzzy-AHP for assigning weights since traditional AHP fails to accommodate both fuzziness and uncertainty [44]. In this study, an FFS map was created using a variety of information, including historical fire reports and an analysis of secondary data obtained from various physiographic, meteorological, and anthropogenic data sources. This study aimed to (i) evaluate and depict forest fire susceptibility (FFS) in the IWH region through the utilization of a GIS-based Fuzzy-AHP technique, and (ii) perform an analysis of forest fire susceptibility based on forest type and district within the IWH region. The evaluation involved quantifying the impact of physiographic, meteorological, and anthropogenic factors on forest fires, with the assignment of weights determined by their relevance in susceptibility estimation. The receiver operating characteristic (ROC) curve and the area under the curve (AUC) were utilized to assess the performance of the proposed model. Ultimately, the findings of this research hold significant implications for estimating the potential environmental consequences of fires. This empowers researchers and decision makers to formulate appropriate post-fire restoration strategies and prioritize conservation efforts.

2. Materials and Methods

2.1. Study Area

This study was conducted for the three Indian Himalayan states of Jammu and Kashmir (JK), Himachal Pradesh (HP), and Uttarakhand (UK), which collectively span 151,382 km^2 of the Indian Western Himalayas (IWH) region and constitute 4.6% of the country's total area. This study area (Figure 1) extends between 73°26′E and 81°01′E and between 28°44′N and 36°58′N. Using the Köppen climate classification, most of the IWH region has a subtropical highland climate (Cwb), and the average temperature ranges from 37 °C in summers to 2.2 °C in winters, with the warmest months being March to June (pre-monsoon). The monsoon season, which lasts from July to September, accounts for the majority of the annual rainfall, which ranges from 600 to 2000 mm. Altitude in this region ranges from 187 m to more than 7000 m. The Pir Panjal Range, Dhauladhar Range, Zanskar Range, and the Great Himalayas are just a few of the notable mountain ranges that make up the Western Himalayas. These mountain ranges are made up of high peaks, jagged summits, and deep valleys. This altitudinal variation results in the formation of a specific pattern of vegetation that includes subtropical woods, conifer mountain forests, alluvial grasslands, and alpine meadows. One of the world's mega-biodiversity hotspots, this area is the habitat for half of India's native plant species and one-tenth of the world's higher-altitude plant and animal species; however, many of the species are yet to be thoroughly studied [45].

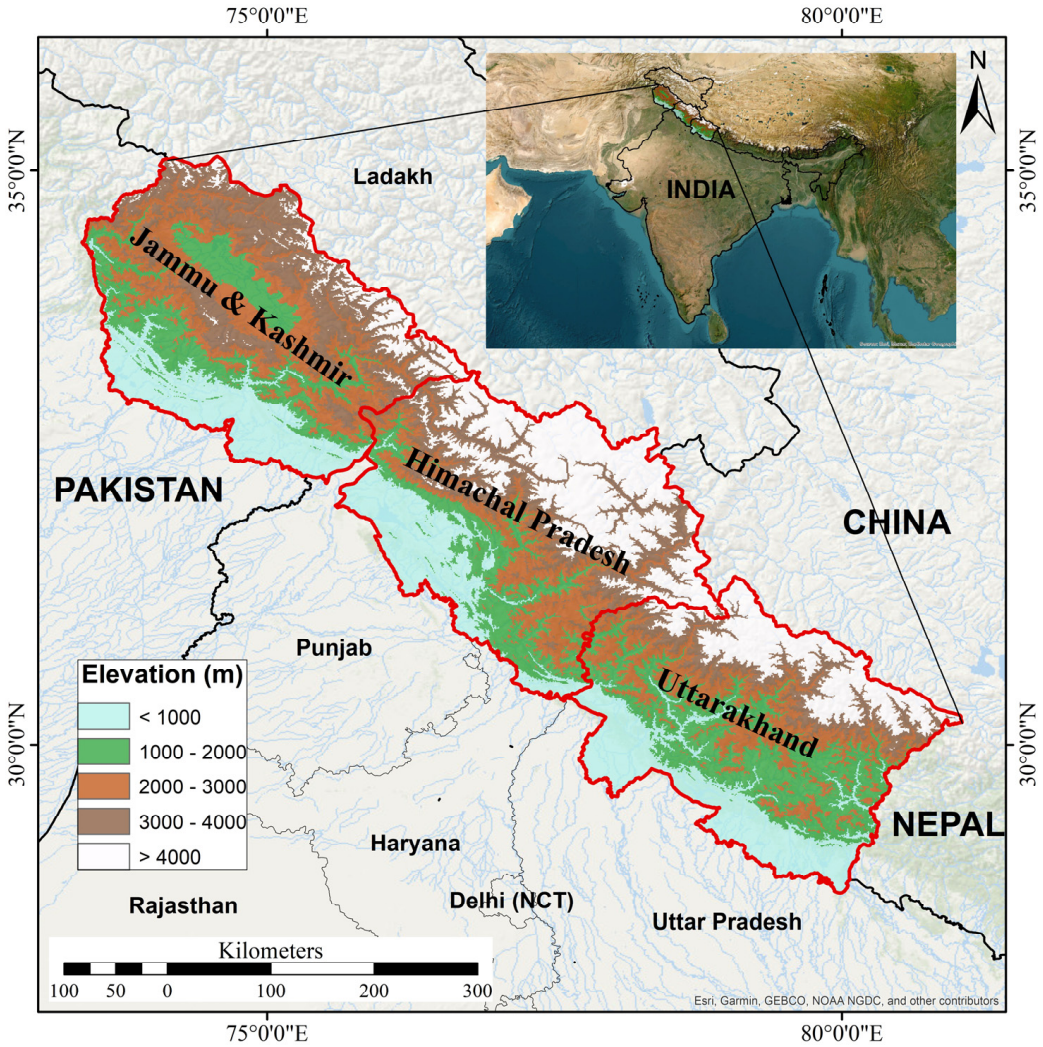

Figure 1. Location of the study area.

The IWH region experiences a fire season that lasts from February to June, peaking in May. Data from Global Forest Watch shows that between 2001 and 2021, wildfires in the Himalayas destroyed more than 35,000 hectares of forest cover. The overall area of forest that was partially or completely burned increased from over 7,200,000 hectares to more than 7,300,000 hectares between 2011 and 2020, according to an analysis of the data. For this reason, probability- or susceptibility-based fire occurrence modeling and future forecasting are crucial for this delicate mountain ecology [13].

2.2. Methodology

The methodology of this work comprised (1) the selection of meteorological, physiographic, and anthropogenic parameters, (2) the use of a GIS-based fuzzy analytical hierarchy process (Fuzzy-AHP) approach, and (3) map validation using the area under the curve (AUC) method. This whole process aimed to assess and map the FFS of the Indian Western Himalayas (IWH) region of India. All the necessary data were gathered from a number of sources, and a thorough description of the data is given in Table 1. Data were prepared and analyzed using ArcGIS, SPSS, and MS-Office, and the resulting information was shown as an FFS map. Figure 2 provides an understanding of the general methodology of this study.

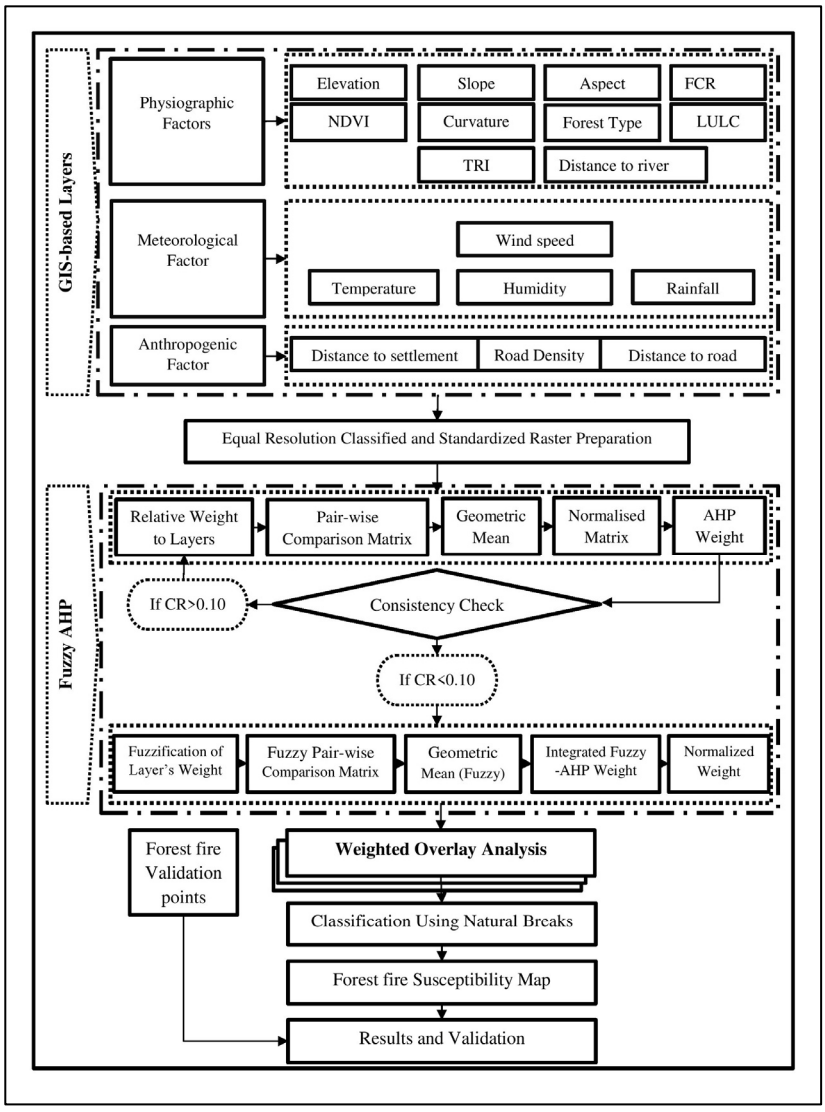

Figure 2. Flowchart representing the complete process of the methodology.

Table 1. Comprehensive database table summarizing the relevant data.

Factors	Data Layer	Resolution/ Scale	Preparation Method	Relation to Forest Fire Susceptibility	Data Source	Period
Physiographic Factors	Elevation	30 m × 30 m	DEM Classification	Negative relation	SRTM Plus V3 (https://earthexplorer.usgs.gov/, accessed on 20 October 2022)	2013
	Slope		Spatial analysis using slope, aspect, and curvature tools	Positive relation		
	Aspect			South-facing more susceptible and vice versa		
	Curvature			Negative relation		
	Distance to river		Euclidean distance	Positive relation		
	TRI		Calculating map algebra using raster calculator	Positive relation		
	NDVI	1000 m	Downloaded, mosaiced, clipped, and averaged	Positive relation	MODIS Vegetation Indices- V6 (https://earthexplorer.usgs.gov/, accessed on 25 October 2022)	2020–2021
	LULC	10 m × 10 m	Clipped from World LULC Database	Positive relation	SENTINEL 2A (https://www.arcgis.com/home/item.html?id=d3da5dd386d140cf93fc9ecbf8da5e31, accessed on 4 November 2022)	2020
	FCR			Positive relation		
	Forest type		Digitized from the obtained data	Positive relation	Wikimedia Commons (https://commons.wikimedia.org/wiki/File:Forest_type_areas_by_counties,_Minnesota,_1962_(IA_foresttypeareasb55chas).pdf, accessed on 5 November 2022)	
Meteorological Factors	Temperature	0.5° × 0.5°	10 years gridded data interpolation using IDW	Positive relation	CRU TS v. 4.07 (https://crudata.uea.ac.uk/cru/data/hrg/cru_ts_4.07/cruts.2304141047.v4.07/pre/, accessed on 11 November 2022)	2011–2020
	Mean annual rainfall			Negative relation		
	Wind speed	375 m	Downloaded and clipped	Negative relation	Global Wind Atlas (https://globalwindatlas.info/en accessed on 16 Novomber 2022)	2020
	Humidity	0.5° × 0.62°	10 years gridded data interpolation using IDW	Positive relation	POWER Data Access Viewer (https://power.larc.nasa.gov/data-access-viewer/ accessed on 22 November 2022)	2011–2020
Anthropogenic Factor	Distance to settlement	10 m × 10 m	Clipped from World LULC Database	Negative relation	SENTINEL 2A (https://www.arcgis.com/home/item.html?id=d3da5dd386d140cf93fc9ecbf8da5e31, accessed on 4 November 2022)	
	Distance to road		Euclidean distance		DIVA GIS (https://www.diva-gis.org/datadown, accessed on 29 November 2022)	
	Road density		Density tool	Positive relation		
Ancillary Data	State outline Uttarakhand Himachal Pradesh J & K	1:1,000,000	Downloaded and merged internal polygons		SOI (https://onlinemaps.surveyofindia.gov.in/Digital_Product_Show.aspx, accessed on 15 October 2022)	

2.2.1. Forest Fire Driving Forces

Physiographic Factors

Elevation

According to [45], the Indian Western Himalayas, which include the states of Uttarakhand, Himachal Pradesh, and Jammu and Kashmir, range in elevation from 187 m to 7383 m. The composition and availability of fuels, such as vegetation and dead biomass, can vary with elevation due to changes in climate, rainfall patterns, and vegetation types. Higher elevations tend to have cooler temperatures, with the temperature falling by 6.5 °C per 1000 m, and higher humidity, which can limit fire spread, while lower elevations with higher temperatures and lower humidity are more susceptible to rapid fire growth and spreading [46–48].

Slope

Slopes can influence the direction of fire spread. Fires generally tend to spread more rapidly on up slopes than down slopes [49]. Steep slopes can accelerate the spread of fire by enhancing the upward movement of heated air and producing a chimney effect. Preheating of fuels owing to radiant heat from flames increases as slope increases, resulting in faster combustion rates and more intense fires [49]. The landforms of the western Himalayas, which are a result of localized earthquake activity, continuous uplift, river erosion, and tectonic pressures, have a particular type of slope that is characterized by steep inclines, rough terrain, deep valleys, and small gorges [50].

Aspect

The Himalayas, being in the northern hemisphere, receive more direct solar radiation on their south-facing slopes. As a result, these slopes tend to have vegetation that is more adapted to warmer and drier conditions, such as grasses and shrubs. In contrast, the north-facing slopes often support more moisture-loving vegetation such as coniferous forest. South-facing vegetations are more flammable and contribute to the spread of forest fires also because of higher temperatures and drier conditions as compared to north-facing slopes [13,51].

Curvature

The concept of curvature pertains to the quantification of the extent to which a surface deviates from being planar [52]. There are two types of curvature of a terrain used in GIS. The first one is plan curvature. This orientation is perpendicular to the steepest slope direction and impacts the way flow converges and diverges across the surface. A positive value indicates lateral convexity of the surface at a specific location, whereas a negative value signifies lateral concavity at that spot. A value of zero denotes a linear surface [53]. The second measure is profile curvature, aligned parallel to the steepest slope direction. A negative value indicates a downward convexity of the surface at a specific location, whereas a positive value signifies upward concavity. A value of zero implies a linear surface. Profile curvature plays a role in affecting the acceleration or deceleration of flow across the surface [53].

Curvature of the land can impact how fire behaves by changing the way wind moves, affecting the amount of fuel present, and influencing the speed at which the fire spreads. When considering the direction and speed of the wind, convex slopes (curving outward) cause the wind to diverge and accelerate, potentially causing the fire to spread faster. In contrast, concave slopes (curving inward) can cause the wind to converge and decelerate, leading to different fire behavior. In terms of fuel accumulation and distribution, convex slopes tend to accumulate fuel due to the collection of debris, which can result in more intense fires.

Distance to River

Rivers can act as natural firebreaks due to their moisture content. The presence of water and the relatively moist conditions near rivers can create a barrier that hinders the

spread of fires. Vegetation along the riverbanks may also have a different moisture content, which can reduce the availability of flammable materials and act as a natural fuel break, slowing down or stopping the fire's progression. The rivers in the western Himalayas form an intricate network of tributaries. This naturally explains the presence of a significant amount of water in the region, which can act as a savior in the case of a fire.

Topographic Roughness Index (TRI)

The topographic roughness index (TRI) is a measure of the surface roughness of a landscape. It estimates elevation changes within a specific neighborhood, providing information about the terrain's roughness or complexity. The topographic roughness index (TRI) quantifies the extent of elevation variation among neighboring cells in a DEM [54]. Topographical roughness influences the rate at which a fire can spread across the landscape. Steep slopes and rugged terrain can accelerate fire spread, as flames can be aided by upslope winds and the preheating of fuels. Flat or gently sloping terrain, on the other hand, can slow down fire spread. Furthermore, high TRI scores frequently indicate more rugged and difficult terrain. This can obstruct firefighters' access to the location of the fire, slowing reaction times and increasing the risk to firefighting teams.

NDVI

NDVI stands for normalized difference vegetation index. The health and density of the vegetation cover for an area are measured using this index. NDVI can offer important details regarding the state of the vegetation and possible fire risk in the context of mountainous forest fires. Generally, healthy, thick vegetation has a high NDVI rating, indicating a significant amount of chlorophyll and active photosynthesis [55–57]. On the other hand, low NDVI readings could point to places with little vegetation, bare soil, or vegetation stressed because of issues like disease or drought. Low NDVI values in forested mountain regions can indicate less fuel moisture and higher vulnerability to fire ignition and spread during times of heightened fire risk, such as dry seasons or protracted heat waves. NDVI data can be used to determine the intensity of a forest fire after it has occurred. Post-fire areas with significantly lower NDVI values indicate extensive vegetation degradation. This type of data is critical for post-fire recovery and restoration operations. Continuous NDVI monitoring can aid in the early detection of potentially fire-prone locations. Changes in NDVI patterns, particularly during dry seasons, might warn authorities of an increased fire danger and prompt proactive fire prevention responses. NDVI data for the months of April to June of 2020 and 2021 were obtained from MODIS Vegetation Indices—V6.1 which is provided by NASA LPDAAC.

Land Use/Land Cover (LULC)

Changes in LULC significantly affect the occurrence of forest fire. An increase or decrease in the abundance of vegetation and changes in its composition can result in increases or decreases in forest fires. Increased human activities, such as urbanization, infrastructure development, or tourism, can introduce new ignition sources and increase the likelihood of accidental fires. Deforestation is leading to changes in local climate patterns, including temperature and rainfall, which may create dried and narrowed water channels and more fire-prone conditions.

Based on previous studies, it can be stated that water availability is the factor that most decreases the likelihood of forest fires igniting, while the presence of fuels such as dense vegetation, dried leaves, and woods is the factor that most increases the likelihood of forest fires igniting [58–60].

Forest Coverage Ratio (FCR)

The forest coverage ratio, which refers to the proportion of land covered by forests, can influence the amount of fuel available for forest fires [61]. The Indian Himalayan region has a very diverse range of forests. About 62.1% of the land is covered by forests, which come in a range of varieties from subtropical to alpine. These forests are home to a variety

of flora and fauna which include many endemic and endangered species [61]. A higher forest coverage ratio denotes the presence of more biomass and vegetation, both of which serve as possible fire starters. Equation (1) was used to calculate the FCR.

$$FCR = F_a / F_c \quad (1)$$

where F_a is the area of forest in a cell, and F_c is the total area of the cell.

Forest Types

There are five types of forest in the IWH region [62]. These are alpine and subalpine, cold desert, Himalayan moist temperate, subtropical coniferous, and tropical moist deciduous. Diversity in flora leads to variation in the amount of dry or wet fuel available for forest fire. It reflects the five different types of forest with their varying flora species which consequently contribute to forest fires in differing percentages. Sub-tropical coniferous forest is very much prone to forest fire while cold desert, alpine, and subalpine forests are the least prone to it.

Meteorological Factors

Temperature

The northwestern Himalayan peaks normally have dry weather, experiencing average temperatures between 37 °C in the hottest month (June) and 2.2 °C in the coldest month (January), along with significant snowfall. As the temperature rises, the moisture in the soil dries out, leading to vegetation and trees that are flammable. Consequently, the land experiences droughts and is no longer suitable for irrigation or other uses. As temperatures continue to climb and global warming continues, forest fires will occur more frequently in upcoming years.

Rainfall

Increased rainfall generally leads to reduced fire occurrence and size, as it enhances fuel moisture levels and decreases fire ignition potential [63,64]. Conversely, drought conditions associated with lower rainfall levels were found to increase the likelihood of forest fires. The warmest months in the western Himalayas are April, May, and June, which have the least rainfall of the year. As a result, the western Himalayan region experiences a fire season that lasts from February to June, peaking in May.

Wind Speed

Wind speed plays a crucial role in determining the behavior and spread of forest fires in mountainous regions. The interaction between wind and fire can significantly impact fire growth, spread rate, and direction of spread [49]. Higher wind speeds can accelerate the rate at which a fire moves through a forested area. The rate of spread is directly proportional to wind speed up to a certain point, beyond which other factors such as fuel availability and topography become more dominant [65].

Humidity

The relative humidity in the western Himalayan region is never greater than 60%. This suggests that the western Himalayas have less moisture, which keeps the relative humidity (RH) value within the range 60% even during the monsoon season. Relative humidity has an effect on wildfires since it can dampen or dry out potential fuel. Low humidity levels can both temporarily increase the risk of a forest fire and also temporarily dry out vegetative fuels. When the air temperature and dew point temperature are both high, the relative humidity is at its lowest.

Anthropogenic Factors

Distance to Settlement

The western Himalayas are home to many villages. These typically consist of groups of homes, frequently made of wood or stone, placed on terraces or slopes. In most self-sufficient villages, the main sources of income are their agricultural areas, orchards, and livestock rearing. The distance between a settlement and a fire source can influence the speed at which the fire spreads. One study [66] found that as fires moved closer to structures, their rate of spread increased significantly. This is because of the presence of flammable materials in settlements, which may act as additional fuel for the fire.

Distance to Road

The development of roads, clearing vegetation, and the movement of travelers are important factors in forest management and investment. Moreover, the construction of roads establishes a direct interface between substantial human activities and the forest ecosystem, elevating the potential for occurrences of forest fire events.

Road Density

The road density in the western Himalayas varies across different regions, depending on factors such as terrain, accessibility, and development priorities. In some areas, particularly in the more populous and developed regions, road density is relatively higher. These regions include the states of Himachal Pradesh and Uttarakhand, where roads connect various towns, villages, and tourist destinations. Increased human activity, such as recreational use, logging, and construction, is frequently correlated with higher road density. The likelihood of human-caused ignitions fueling forest fires can increase because of these activities.

2.2.2. GIS-Based Fuzzy Analytical Hierarchy Process (Fuzzy-AHP) Approach

The analytical hierarchy process (AHP), devised by [36], is a very successful groupware multi-criteria decision-making process that enables the integration of expert perspectives by breaking down difficult issues across the hierarchical levels. According to published research, AHP has been widely used in academia and industry to solve complex decision-making issues and to determine the weights of criteria that can be combined with other operational or probabilistic techniques. Examples of these techniques include the hybrid AHP-SWOT (strengths, weaknesses, opportunities, and threats) method [67] and the AHP integration with decision tree analysis [68].

The AHP is one of the best multi-criteria approaches for determining where forest fires may start. Numerous research studies have examined evidence for AHP's alleged usefulness against forest fires [69–71]. AHP, however, has several real-world issues. First, as the number of criteria and choices rises, overall performance of the method declines. Second, the method does not provide for justification of the ambiguity in assessors' (experts') subjective judgments. Due to these factors, studies favor the application of fuzzy logic (FL) theory to enhance the mathematical notion of simple AHP [72,73].

Fuzzy analytic hierarchy process (Fuzzy-AHP) is the integration of qualitative and quantitative methods. The Fuzzy-AHP has been gradually improved as a useful technique for handling complications involving decision making. The author of [74] developed fuzzy set theory in 1965, a modeling technique that effectively reflects complicated systems for which crisp numerical explanations are not possible. This method makes use of membership values ranging from 0 to 1, showing the extent of membership, expressing the inherent ambiguity of real-world events [74]. Notably, the concept of fuzzy sets theory has found application in various other MCDA techniques, including fuzzy TOPSIS (technique for order of preference by similarity to ideal solution) [75], and fuzzy PROMETHEE (preference ranking organization method for enrichment of evaluations) [76]. The linguistic expressions utilized in Fuzzy-AHP to conduct pairwise comparisons can be assigned numerical values using the 1–9 scale introduced by Saaty in 1980. The associated conversion scale for

transforming these values into fuzzy numbers representing relative importance is presented in Table 2 [77].

Table 2. Fuzzy scale of the relative importance [77].

Saaty Scale	Definition of Linguistic Terms	Triangular Fuzzy Numbers Scale	Reversed Values	TFN Conversion
1	Equal (EQ)	(1,1,1)	1/1	(1/1, 1/1, 1/1)
3	Moderate (MD)	(2,3,4)	1/3	(1/4, 1/3, 1/2)
5	Strong (ST)	(4,5,6)	1/5	(1/6, 1/5, 1/4)
7	Very Strong (VS)	(6,7,8)	1/7	(1/8, 1/7, 1/6)
9	Extremely Strong (ES)	(9,9,9)	1/9	(1/9, 1/9, 1/9)
2	Intermediate Values	(1,2,3)	1/2	(1/3, 1/2, 1/1)
4		(3,4,5)	1/4	(1/5, 1/4, 1/3)
6		(5,6,7)	1/6	(1/7, 1/6, 1/5)
8		(7,8,9)	1/8	(1/9, 1/8, 1/7)

Mathematical Definitions of Fuzzy Numbers and Membership Function

A collection of fuzzy numbers, denoted as $\tilde{A}$, within a subset X of the real number set R, is established as a set of ordered pairs $\tilde{A} = \{x, \mu\tilde{A}(x)\}$, where x belongs to X and $\mu\tilde{A}(x)$: $X \rightarrow [0, 1]$. The function $\mu\tilde{A}(x)$ is recognized as the membership function for $\tilde{A}$, responsible for assigning a membership grade ranging between 0 and 1 to each element x, signifying its degree of association [74,78]. A normalized fuzzy set has a special case in which the total of the membership values of all its elements is equal to 1. In other words, the membership values are scaled or changed so that they total one [79]. Depending on membership function, there are many kinds of fuzzy numbers, but the triangular and trapezoidal shapes are the most common and useful. Trapezoid fuzzy numbers address more widespread cases of ambiguity in decision-making analysis ideas [80,81]. But triangular fuzzy numbers are preferred over trapezoidal fuzzy numbers due to their inherent simplicity and better interpretability in multi-criteria decision-making problems [82]. Furthermore, the usage of triangular fuzzy numbers frequently results in simpler mathematical computations and streamlined decision algorithms [83]. The triangular fuzzy number is depicted in Figure 3. The triangular fuzzy numbers (TFNs) used in this paper for the FFS zonation of the IWH were given by [72].

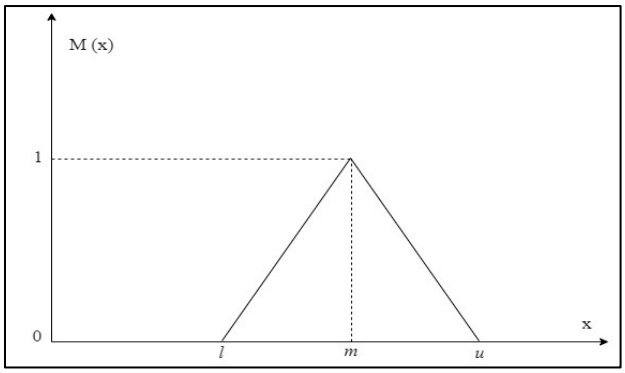

Figure 3. Triangular fuzzy number (TFN).

Figure 3 represents the triangular fuzzy number and Figure 4 is a visual illustration of the membership function (MF) utilized in the current paper to interpret the fuzzy linguistic terms, as put forth by [77].

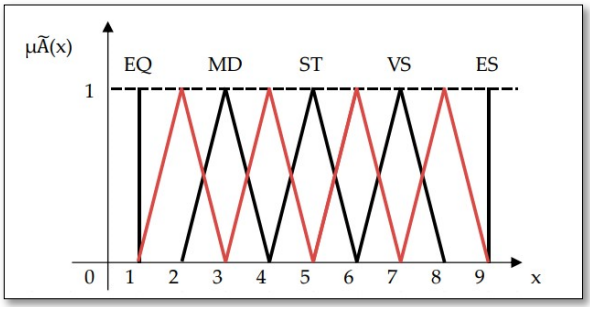

Figure 4. Interpretation of fuzzy linguistic terms [77].

Geometric Mean—Fuzzy-AHP Method

Within this paper, the application of Buckley's Fuzzy-AHP method from 1985 was undertaken to analyze forest fire risk factors and define FFS zones. The entire procedure has been methodically organized and constructed in accordance with the following steps:

Step-1: Establishing the objective, constructing the hierarchical structure, and identifying each risk factor and its corresponding sub-factors.

Step-2: Development of the pairwise comparison matrix, in which the elements [ãij]k represents the kth experts' preference of the risk factor i over the risk factor j; i, j ∈ N. The fundamental relationship between the elements of the reciprocal matrix is (ãij)·(ãji) = 1. If criteria 1–9 are used for the measurement of relative importance of criterion i with respect to criterion j, then values $\widetilde{1}^{-1}, \widetilde{2}^{-1}, \widetilde{3}^{-1}, \widetilde{4}^{-1}, \widetilde{5}^{-1}, \widetilde{6}^{-1}, \widetilde{7}^{-1}, \widetilde{8}^{-1}, \widetilde{9}^{-1}$ represent its reciprocal and the values represent the degree of importance of criterion j relative to criterion i. Description of the fuzzy conversion scale is provided in a study [84].

Step-3: Creating the average pairwise comparison matrix denoted as [a], in which the elements consist of the average values of the preferences of experts, achieved by employing Equation (2):

$$A_{ij} = \frac{\sum\left(\mathrm{aij}^1 + \mathrm{aij}^2 + \ldots + \mathrm{aij}^k\right)}{\mathrm{k}} (\mathrm{k} : \text{number of experts engaged}) \quad (2)$$

Step-4: AHP weight is calculated and validated on the basis of consistency ratio (CR), whether it is less than 0.10 or not. In the second case, the matrix is revised, and further weight is calculated to make sure that the CR is less than 0.10.

Step-5: Construction of fuzzy pairwise comparison matrix denoted as [ã], where the elements are represented by fuzzy values denoted as ãij. These fuzzy values are determined using the linguistic scale of the MF along with the processes of TFN numerical conversion as outlined in Table 2.

Step-6: Estimation of the fuzzy geometric mean value for each risk factor Ri (Equation (3)), according to the approach of [72]:

$$\mathrm{R_i} = \left\{\prod_{\mathrm{j=1}}^{\mathrm{n}} \tilde{\mathrm{A}}_{\mathrm{ij}}\right\}^{1/\mathrm{n}} = \left(\tilde{\mathrm{A}}\mathrm{i1} \otimes \tilde{\mathrm{A}}\mathrm{i2} \otimes \tilde{\mathrm{A}}\mathrm{i3} \otimes \ldots \tilde{\mathrm{A}}\mathrm{in}\right)^{1/\mathrm{n}} \quad (3)$$

Upon determination of geometric means, the vector of fuzzy geometric risk factors is formulated as per Equation (4).

$$\mathrm{R} = [\mathrm{R_1}, \mathrm{R_2}, \mathrm{R_3}, \ldots \mathrm{R_n}]^{\mathrm{T}} \quad (4)$$

Step-7: Defining the fuzzy risk factors, which correspond to the fuzzy relative weights denoted as Wi, in the following manner:

$$\mathrm{W_i} = \tilde{R}_i \otimes \left[\sum_{j=1}^{n} R_j\right]^{-1} = \mathrm{Ri} \otimes (\mathrm{R1} \oplus \mathrm{R2} \oplus \mathrm{R3} \oplus \ldots \oplus \mathrm{Rn}) - 1R \quad (5)$$

Step-8: Converting the fuzzy relative weights W_i into crisp values W_i through the process of de-fuzzification. This is achieved by utilizing the center of the area (CoA) method, using Equation (6).

$$W_i = \frac{L.Wi + M.Wi + U.Wi}{3} \quad (6)$$

Step-9: Standardizing the de-fuzzified relative weights W_i using normalization, carried out by employing Equation (7):

$$W_{Ni} = Wi / \left(\sum_{i=1}^{n} W_i\right) \quad (7)$$

Step-10: All layers are finally combined according to Equation (8) to create the forest fire susceptibility (FFS) zone map.

$$\text{FFS Zones} = \sum_{i=1}^{n} X_i.W_{Ni} \quad (8)$$

where W_{Ni} is the normalized fuzzy weight for the X_i factor.

2.2.3. Validation of Forest Fire Susceptibility Maps

Validation is an essential procedure to determine the effectiveness of the chosen methodology in forest fire vulnerability assessment [6]. The receiver operating characteristic—area under the curve (ROC-AUC) technique is frequently used in accuracy assessment of various MCDM techniques, and because of its adaptability and efficacy in capturing the degree of vulnerability, this approach is preferred for assessing the accuracy of used models. In the current study, this approach was used for assessing the effectiveness of Fuzzy-AHP in FFS zonation. The ROC curve is a visual tool for evaluating the trade-off between specificity and sensitivity (calculated according to Equations (9) and (10)), with the *x*-axis showing a false-positive rate (specificity) and the *y*-axis showing a true-positive rate (sensitivity) to judge the accuracy of the model's predicting ability [85].

$$\text{Sensitivity} = \frac{TP}{TP + FN} \quad (9)$$

$$\text{Specificity} = \frac{TN}{FP + TN} \quad (10)$$

where TP: true positive; TN: true negative; FP: false positive; FN: false negative.

3. Results

3.1. Preparation of the Spatial Databases

The drivers, or forest fire conditioning factors, used in this study to map FFS in the western Himalayas consisted of physiographic, meteorological, and anthropogenic parameters. The spatial data layers of these parameters were compiled in ArcGIS from the sources listed in Table 1.

The physiographic factors, including elevation, slope, aspect, curvature, distance to river, and TRI (Figure 5a–f), were extracted from the SRTM-DEM. The IWH is characterized by a 7–7383 m elevation range, with a mean elevation of 2528.16 m; a 0°–46.67° slope range dominated by steeper slopes of 11.75°; south- and southwest-facing slope aspects; and a (−0.008111)–(0.00455) curvature. Moreover, the maximum distance of a location to a river was found to be 30.92 km, and the IWH is dominated by a TRI range of 0.42–0.58. The NDVI map of the region (Figure 5g) was extracted from MODIS Vegetation Indices-V6 data, and the IWH has a mean NDVI of 0.25. The LULC map (Figure 5h) was extracted from the World LULC Database, which uses Sentinel-2A data, and it is evident that the IWH has significant area under forest cover. The FCR map of the IWH (Figure 5i) was created on the basis of areal expanses of forests in the LULC map according to the Equation (1). The forest type map of the IWH (Figure 5j) was digitized from a Wikimedia Commons (2021) map. The IWH consists of five types of forests, including the area-dominating alpine

and subalpine forests, Himalayan moist temperate forests, subtropical coniferous forests, tropical moist deciduous forests, and the cold desert areas.

The meteorological factors included in this study include temperature, mean annual rainfall, wind speed, and humidity. The temperature and mean annual rainfall data layers (Figure 5k–l) were developed from global gridded data (0.5° × 0.5°) of the Climate Research Unit, University of East Anglia. Annual rainfall and temperature for the IWH average 940.6 mm and 12.78 °C, respectively. The wind speed map (Figure 5m) was created from Global Wind Atlas data of 375 m resolution. On average, wind speeds of less than 2 ms-1 dominate across the IWH, except in the higher reaches of the Himalayan ranges where friction and obstruction are the lowest. A humidity map of the IWH (Figure 5n) was prepared from the global gridded data (0.5° × 0.62°) of NASA POWER, and the map shows that humidity in the IWH ranges between 3.07–10.79%.

The data layers for the anthropogenic factors were prepared as follows. The distance-to-settlement map (Figure 5o) was prepared using built-up areas extracted from LULC using the Euclidean distance tool. The distance-to-road map (Figure 5p) was created from the Roads shapefile downloaded from the DIVA GIS Portal using Euclidean distance, and the road density map was prepared using the line density tool.

The data layers of all the aforementioned drivers were converted into raster data layers and resampled to the spatial resolution of 1000 m. These factor maps were classified into sub-classes so that the differential influence of these classes on the occurrence of fire incidents could be ranked. The factors, including elevation, slope, curvature, distance to river, TRI, NDVI, temperature, mean annual rainfall, humidity, road density, distance to road, and distance to settlement, were classified into five classes by quantile method as this method assigns the same number of data values to each class and represents the maximum spatial variation of a geographical attribute. The wind speed map was classified into five classes by the defined interval method, while aspect, LULC, and forest type, and have the predefined classification schemes. The classification of FCR, intended to be divided into two distinct groups, was done by the equal interval approach to categorize the data based on the central value.

3.2. Forest Fire Susceptibility (FFS) Mapping

In this study, seventeen drivers that influence the forest fire were considered to study FFS in the IWH. The factors categorized into physiographic, meteorological, and anthropogenic factors were separately subjected to the Fuzzy-AHP process.

Firstly, to determine the relative importance of the factors in conditioning forest fires in the Himalayan region, ordinal ranks of the factors (Table 3) were determined based on the knowledge of the group of decision makers (GDM). The GDM unanimously ranked the physiographic factors from 1 to 10, suggesting that the influence of the physiographic factors descended in the order FCR > NDVI > forest type > distance to river > LULC > slope > TRI > elevation > curvature > aspect. Similarly, the meteorological factors and anthropogenic factors were ranked in the ranges of 1 to 4 and 1 to 3, respectively. The role of meteorological factors decreased in the order temperature > wind speed > humidity > rainfall, and that of anthropogenic factors decreased in the order distance to settlement > road density > distance to road.

Secondly, the ranks of the sub-classes of the drivers were determined by the GDM on the basis of trends of susceptibility followed by the factor sub-classes. The numerical ordering ranks were assigned unanimously such that the least important sub-class of a factor was ranked 0 or 1, with increasing ranks for subsequent numerical ranks. Table 4 represents the ordinal ranking of the sub-classes of the drivers.

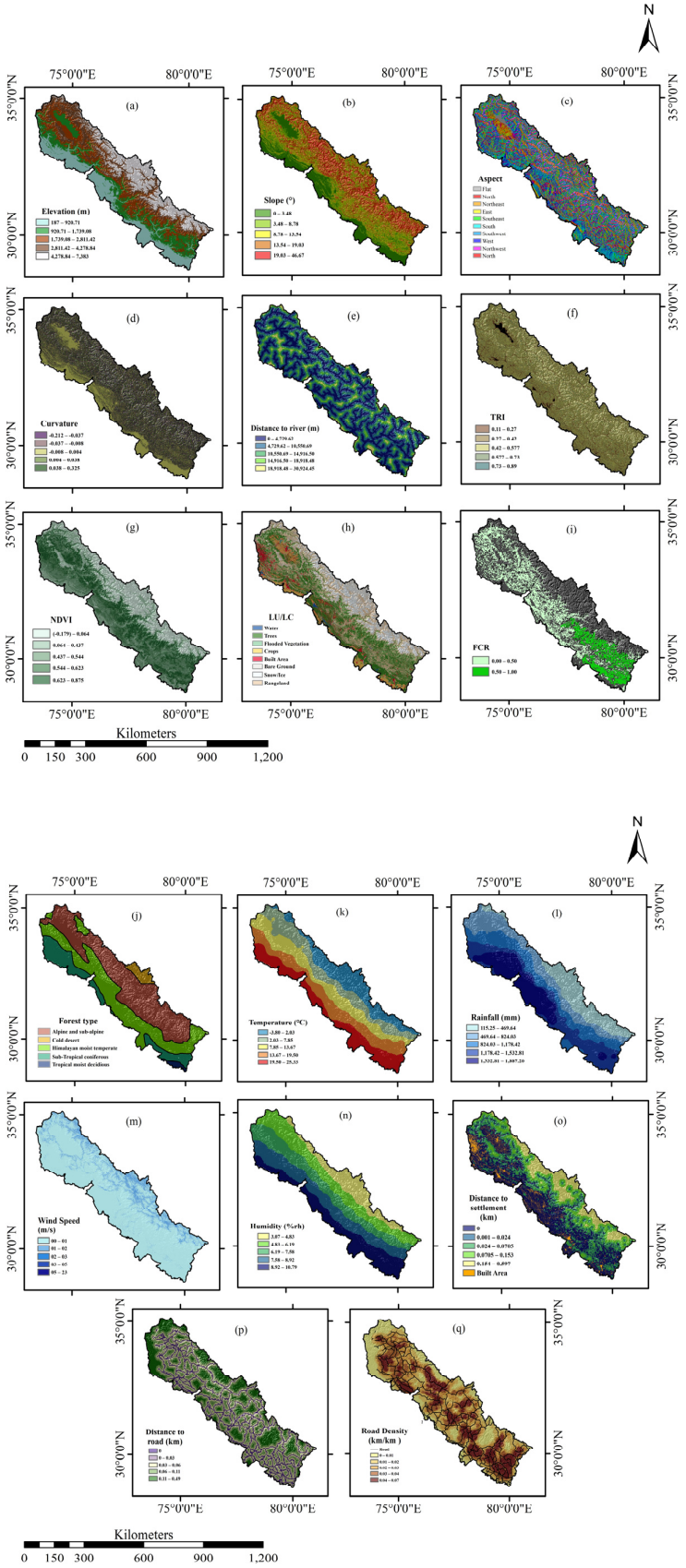

Figure 5. Forest fire drivers: (**a**) elevation; (**b**) slope; (**c**) aspect; NDVI; (**d**) curvature; (**e**) distance to river; (**f**) TRI; (**g**) NDVI; (**h**) LULC; (**i**) FCR; (**j**) forest type; (**k**) temperature; (**l**) rainfall; (**m**) wind speed; (**n**) humidity; (**o**) distance to settlement; (**p**) distance to road; (**q**) road density.

Table 3. Rankwise ordering of the drivers.

Factor Category	Drivers	Order
Physiographic factors	FCR	1
	NDVI	2
	Forest Type	3
	Distance to River	4
	LULC	5
	Slope	6
	TRI	7
	DEM	8
	Curvature	9
	Aspect	10
Meteorological factors	Temperature	1
	Wind speed	2
	Humidity	3
	Rainfall	4
Anthropogenic factors	Distance to Settlement	1
	Road Density	2
	Distance to Road	3

Table 4. Weights for the sub-classes of meteorological, physiographic, and anthropogenic factors.

Factors	Sub-Classes	Class Interval	Rank
Physiographic Factors	**Elevation**	187–920.709804	5
		920.709804–1739.078431	4
		1739.078431–2811.423529	3
		2811.423529–4278.843137	2
		4278.843137–7383	1
	Slope	0–3.477381	4
		3.477381–8.784962	4
		8.784962–13.543483	3
		13.543483–19.034084	2
		19.034084–46.670109	1
	Aspect	Flat	1
		North	2
		Northeast	3
		East	4
		Southeast	5
		South	6
		Southwest	5
		West	4
		Northwest	3
		North	2

Table 4. *Cont.*

Factors	Sub-Classes	Class Interval	Rank
Physiographic Factors	**Curvature**	(−0.2128)–(−0.037654)	1
		(−0.037654)–(−0.008111)	2
		(−0.008111)–(0.00455)	3
		0.00455–0.038313	2
		0.038313–0.3253	1
	Distance to River	0–3274.353033	1
		3274.353033–6669.978401	2
		6669.978401–9944.331434	3
		9944.331434–13825.04614	4
		13825.04614–30924.445313	5
	TRI	0.111084–0.266644	1
		0.266644–0.422205	2
		0.422205–0.577765	3
		0.577765–0.733325	4
		0.733325–0.888885	5
	NDVI	(−0.1793)–(0.064559)	1
		0.064559–0.436547	2
		0.436547–0.54401	3
		0.54401–0.622541	4
		0.622541–0.874667	5
	LULC	Water	1
		Trees	7
		Flooded Vegetation	2
		Crops	6
		Built Area	5
		Bare Ground	4
		Snow/Ice	1
		Rangeland	3
	FCR	1	1
		0	0
	Forest Type	Alpine and subalpine	2
		Cold desert	1
		Himalayan moist temperate	3
		Sub-tropical coniferous	4
		Tropical moist deciduous	5
Meteorological Factors	**Temperature**	(−3.800027)–(2.026002)	1
		2.026002–7.852031	2
		7.852031–13.67806	3
		13.67806–19.504089	4
		19.504089–25.330118	5

Table 4. *Cont.*

Factors	Sub-Classes	Class Interval	Rank
Meteorological Factors	**Wind speed**	0–1	1
		01–02	2
		02–03	3
		03–05	4
		05–23	5
	Humidity	3.074757–4.830578	5
		4.830578–6.192852	4
		6.192852–7.5854	3
		7.5854–8.917402	2
		8.917402–10.794313	1
	Rainfall	115.253502–469.642621	5
		469.642621–824.03174	4
		824.03174–1178.420859	3
		1178.420859–1532.809978	2
		1532.809978–1887.199097	1
Anthropogenic Factors	**Distance to Settlement**	0	5
		0–0.023484	4
		0.023484–0.070453	3
		0.070453–0.152649	2
		0.152649–0.598854	1
	Road Density	0–0.012692	1
		0.012692–0.021154	2
		0.021154–0.027077	3
		0.027077–0.033564	4
		0.033564–0.071923	5
	Distance to Road	0	5
		0–0.025008	4
		0.025008–0.055786	3
		0.055786–0.113496	2
		0.113496–0.490533	1

Thirdly, in accordance with the TFN scale given in Table 2 and the subjective judgment of the GDM, separate pairwise comparison matrices of the physiographic factors (Table 5), meteorological factors (Table 6), and anthropogenic factors (Table 7) were developed. Using these pairwise comparison matrices, the geometric mean of each driver was calculated using Equation (5), followed by calculation of the fuzzy weights according to Equation (6). The fuzzy weights thus derived were de-fuzzified using the center of area method given in Equation (7) to determine the final normalized weights of each conditioning factor. The geometric mean, fuzzy weights, and normalized weights of all the drivers are given along with their respective pairwise comparison matrix tables.

Table 5. Pairwise comparison matrix (physiographic factors).

Factors	FCR			NDVI			Forest Type			Distance to River			LULC			Slope		
FCR	**1.00**	**1.00**	**1.00**	1.00	2.00	3.00	3.00	4.00	5.00	3.00	4.00	5.00	3.00	4.00	5.00	3.00	4.00	5.00
NDVI	0.33	0.50	1.00	**1.00**	**1.00**	**1.00**	1.00	2.00	3.00	3.00	4.00	5.00	3.00	4.00	5.00	3.00	4.00	5.00
Forest Type	0.20	0.25	0.33	0.33	0.50	1.00	**1.00**	**1.00**	**1.00**	1.00	2.00	3.00	2.00	3.00	4.00	2.00	3.00	4.00
Distance to River	0.20	0.25	0.33	0.20	0.25	0.33	0.33	0.50	1.00	**1.00**	**1.00**	**1.00**	1.00	1.00	2.00	1.00	2.00	3.00
LULC	0.20	0.25	0.33	0.20	0.25	0.33	0.25	0.33	0.50	0.50	1.00	1.00	**1.00**	**1.00**	**1.00**	1.00	2.00	3.00
Slope	0.20	0.25	0.33	0.20	0.25	0.33	0.25	0.33	0.50	0.33	0.50	1.00	0.33	0.50	1.00	**1.00**	**1.00**	**1.00**
TRI	0.14	0.17	0.20	0.17	0.20	0.25	0.20	0.25	0.33	0.20	0.25	0.33	0.25	0.33	0.50	0.33	0.50	1.00
DEM	0.13	0.14	0.17	0.14	0.17	0.20	0.17	0.20	0.25	0.17	0.20	0.25	0.20	0.25	0.33	0.25	0.33	0.50
Curvature	0.13	0.14	0.17	0.14	0.17	0.20	0.17	0.20	0.25	0.17	0.20	0.25	0.20	0.25	0.33	0.25	0.33	0.50
Aspect	0.13	0.14	0.17	0.14	0.17	0.20	0.17	0.20	0.25	0.17	0.20	0.25	0.20	0.25	0.33	0.25	0.33	0.50

TRI			DEM			Curvature			Aspect			Geometric Mean			Fuzzy Weight			Normalized Weight
5.00	6.00	7.00	6.00	7.00	8.00	6.00	7.00	8.00	6.00	7.00	8.00	**3.12**	**4.00**	**4.82**	**0.29**	**0.28**	**0.26**	**0.28**
4.00	5.00	6.00	5.00	6.00	7.00	5.00	6.00	7.00	5.00	6.00	7.00	**2.32**	**3.05**	**3.88**	**0.21**	**0.21**	**0.21**	**0.21**
3.00	4.00	5.00	4.00	5.00	6.00	4.00	5.00	6.00	4.00	5.00	6.00	**1.48**	**2.02**	**2.65**	**0.14**	**0.14**	**0.14**	**0.14**
3.00	4.00	5.00	4.00	5.00	6.00	4.00	5.00	6.00	4.00	5.00	6.00	**1.10**	**1.41**	**1.93**	**0.10**	**0.10**	**0.11**	**0.10**
2.00	3.00	4.00	3.00	4.00	5.00	3.00	4.00	5.00	3.00	4.00	5.00	**0.88**	**1.23**	**1.56**	**0.08**	**0.09**	**0.08**	**0.08**
1.00	2.00	3.00	2.00	3.00	4.00	2.00	3.00	4.00	2.00	3.00	4.00	**0.62**	**0.88**	**1.27**	**0.06**	**0.06**	**0.07**	**0.06**
1.00	**1.00**	**1.00**	2.00	3.00	4.00	2.00	3.00	4.00	2.00	3.00	4.00	**0.48**	**0.63**	**0.84**	**0.04**	**0.04**	**0.05**	**0.04**
0.25	0.33	0.50	**1.00**	**1.00**	**1.00**	2.00	3.00	4.00	2.00	3.00	4.00	**0.35**	**0.43**	**0.56**	**0.03**	**0.03**	**0.03**	**0.03**
0.25	0.33	0.50	0.25	0.33	0.50	**1.00**	**1.00**	**1.00**	2.00	3.00	4.00	**0.28**	**0.35**	**0.45**	**0.03**	**0.02**	**0.02**	**0.02**
0.25	0.33	0.50	0.25	0.33	0.50	0.25	0.33	0.50	**1.00**	**1.00**	**1.00**	**0.23**	**0.28**	**0.37**	**0.02**	**0.02**	**0.02**	**0.02**

Table 6. Pairwise comparison matrix (meteorological factors).

Factors	Temperature			Wind Speed			Humidity			Rainfall			Geometric Mean			Fuzzy Weight			Normalized Weight
Temperature	**1.00**	**1.00**	**1.00**	2.00	3.00	4.00	3.00	4.00	5.00	4.00	5.00	6.00	**2.21**	**2.78**	**3.31**	**0.53**	**0.53**	**0.51**	**0.52**
Wind Speed	0.25	0.33	0.50	**1.00**	**1.00**	**1.00**	2.00	3.00	4.00	4.00	5.00	6.00	**1.19**	**1.50**	**1.86**	**0.28**	**0.28**	**0.29**	**0.28**
Humidity	0.20	0.25	0.33	0.25	0.33	0.50	**1.00**	**1.00**	**1.00**	1.00	2.00	3.00	**0.47**	**0.64**	**0.84**	**0.11**	**0.12**	**0.13**	**0.12**
Rainfall	0.17	0.20	0.25	0.16	0.20	0.25	0.33	0.50	1.00	**1.00**	**1.00**	**1.00**	**0.31**	**0.38**	**0.50**	**0.07**	**0.07**	**0.08**	**0.07**

Table 7. Pairwise comparison matrix (anthropogenic factors).

Factors	Distance to Settlement			Road Density			Distance to Road			Geometric Mean			Fuzzy Weight			Normalized Weighted
Distance to Settlement	**1.00**	**1.00**	**1.00**	3.00	4.00	5.00	4.00	5.00	6.00	**2.29**	**2.71**	**3.11**	**0.70**	**0.68**	**0.66**	**0.68**
Road Density	0.20	0.25	0.33	**1.00**	**1.00**	**1.00**	1.00	2.00	3.00	**0.58**	**0.79**	**1.00**	**0.18**	**0.20**	**0.21**	**0.20**
Distance to Road	0.17	0.20	0.25	0.33	0.50	1.00	**1.00**	**1.00**	**1.00**	**0.38**	**0.46**	**0.63**	**0.12**	**0.12**	**0.13**	**0.12**

Table 8. Pairwise comparison matrix (all factors).

Factors	Anthropogenic			Physiographic			Climatic			Geometric Mean			Fuzzy Weight			Avg Fuzzy
Anthropogenic	**1.00**	**1.00**	**1.00**	1.00	2.00	3.00	2.00	3.00	4.00	**1.26**	**1.82**	**2.29**	**0.53**	**0.54**	**0.51**	**0.52**
Physiographic	0.33	0.50	1.00	**1.00**	**1.00**	**1.00**	1.00	2.00	3.00	**0.69**	**1.00**	**1.44**	**0.29**	**0.30**	**0.32**	**0.30**
Climatic	0.25	0.33	0.50	0.33	0.50	1.00	**1.00**	**1.00**	**1.00**	**0.44**	**0.55**	**0.79**	**0.18**	**0.16**	**0.18**	**0.17**

The normalized weights of the physiographic factors, given in Table 5, were integrated with their respective raster data layers in the ArcGIS, and the layers were then combined in accordance with Equation (8) to synthesize the physiographic FFS map of the IWH (Figure 6a). Similarly, the meteorological and anthropogenic FFS maps (Figure 6b,c) were synthesized on the basis of the normalized weights of the drivers given in Tables 6 and 7, respectively.

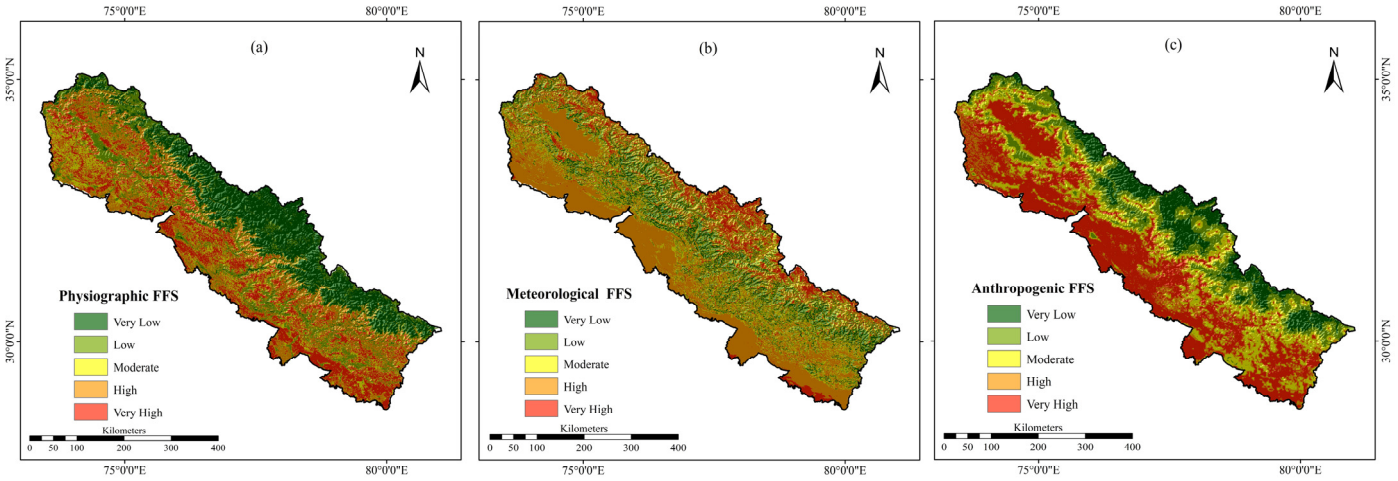

Figure 6. Forest fire susceptibility (FSS): (**a**) physiographic FSS, (**b**) meteorological FSS, (**c**) anthropogenic FSS.

Using the physiographic, meteorological, and anthropogenic FFS maps of the IWH as factors, an overall FFS map was synthesized using the pairwise comparison matrix of geometric means, fuzzy weights, and normalized weights given in Table 8, as determined by the Fuzzy-AHP method. The overall FFS map was classified into five zones from very low fire susceptibility (VL) to very high fire susceptibility (VH) using the quantile method. The classified map is shown in Figure 7. The map shows that 50,693 km^2 (22.66%) of the IWH falls in the very high FFS zone; 57,494 km^2 (25.7%) in the high susceptibility zone; 37,385 km^2 (16.71%) in the medium susceptibility zone; 39,200 km^2 (17.52%) in the low susceptibility zone; and 38,954 km^2 (17.41%) in the very low susceptibility zone.

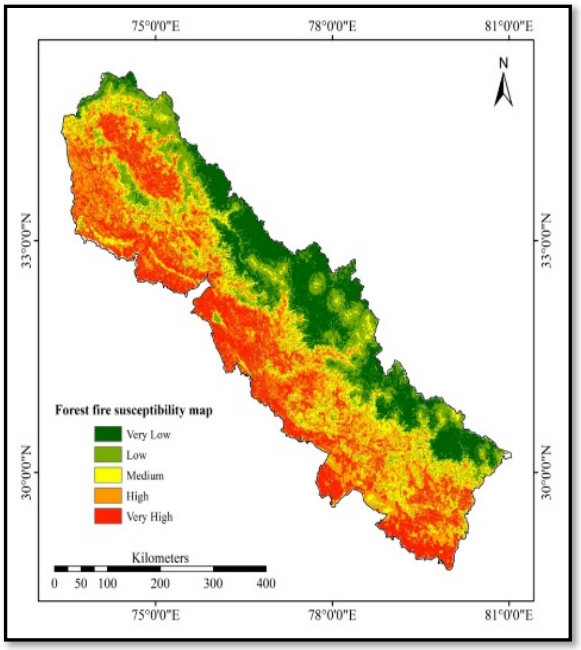

Figure 7. FFS map with varying intensities of fire susceptibility.

3.3. Map Validation Using ROC-AUC

The validation of the FFS map generated through the GIS-based Fuzzy-AHP approach was conducted using receiver operating characteristic–area under curve (ROC-AUC) analysis. A total of 790 true positive data points were extracted from the Visible Infrared Imaging Radiometer Suite (S-NPP/VIIRS) at a 375 m resolution for the years 2011 and 2022 (depicted in Figure 8a). Based on the assumption that the snow, water bodies, flooded vegetation, and rangeland classes of the land use/land cover (LU/LC) map lack the fuels for forest fire, an equal number of true negative points were derived from the snow, water bodies, flooded vegetation, and rangeland classes of the land use/land cover (LU/LC) map.

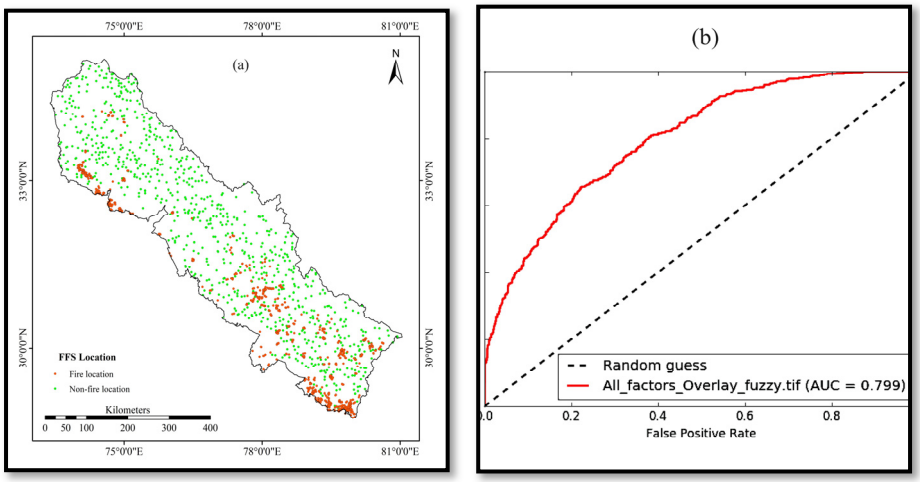

Figure 8. (**a**) Validation points for FFS; (**b**) ROC-AUC curve.

The resulting FFS map, produced as part of this study, demonstrated a predictive accuracy of 79.9%. This accuracy level indicates a substantial agreement between the projected and observed FFS, as illustrated in Figure 8b. This outcome underscores the efficacy of the methodology employed, which involved assigning weights to different meteorological, physiographic, and anthropogenic parameters. Through this approach, the research successfully captured and conveyed the genuine FFS across the entire study area.

3.4. Analysis of the Vulnerability to Forest Fires by Forest Type

The vulnerability of various forest types of the IWH to forest fires is summarized in Table 9 and depicted in Figure 9. Among the five different forest types of the IWH, the tropical moist deciduous forest cover is highly prone to forest fire with 86.85% of its area in a very high FFS zone, 12% in a high FFS zone, 1.15% in a medium FFS zone, and no area the low and very low FFS zones. Subtropical coniferous forest ranked second in vulnerability to forest fire with 47.84%, and 41.29% in the very high and high FFS zones. Only 9.76% and 1.11% of these forests were in the medium and low FFS zones, with no area in the very low FFS zone. The Himalayan moist temperate forests in the IWH ranked third in vulnerability to forest fire with 30.01%, 34.04%, 20.01%, 12.16%, and 3.79% of their area in very high, high, medium, low, and very low FFS zones, respectively. Alpine and subalpine forests are relatively less vulnerable, as 9.64%, 16.76%, and 17.81% of these forests fall in the very high, high, and medium FFS zones of the IWH. Moreover, 29.57% and 26.22% of these forests fall in the very low and low FFS zones, indicating their relative invulnerability. The cold desert has the highest percentage of area in the very low FFS zones (70.51%), followed by its area in low FFS zones (28.01%), medium FFS zones (1.39%), and less than 1% in the high and very high FFS zones. This indicates that the region spanned by the cold desert is immune to forest fire. As per these results, the forest fire vulnerability of different forest types in the IWH was ranked in the order tropical moist deciduous forest > subtropical coniferous > Himalayan moist temperate > alpine and subalpine > cold desert. Since the distribution

of these forests is regulated primarily by the elevation, it was determined that there is a strong influence of topography, especially elevation, on the FFS.

Table 9. Percentage of area of each forest type under the varying intensities of FFS.

Forest Type	Very Low	Low	Medium	High	Very High
Cold desert	**70.52**	**28.01**	**1.39**	**0.08**	**0.00**
Alpine and subalpine	**29.57**	**26.22**	**17.81**	**16.76**	**9.64**
Himalayan moist temperate	**3.79**	**12.16**	**20.01**	**34.04**	**30.01**
Subtropical coniferous	**0.00**	**1.11**	**9.76**	**41.29**	**47.84**
Tropical moist deciduous	**0.00**	**0.00**	**1.15**	**12.00**	**86.85**

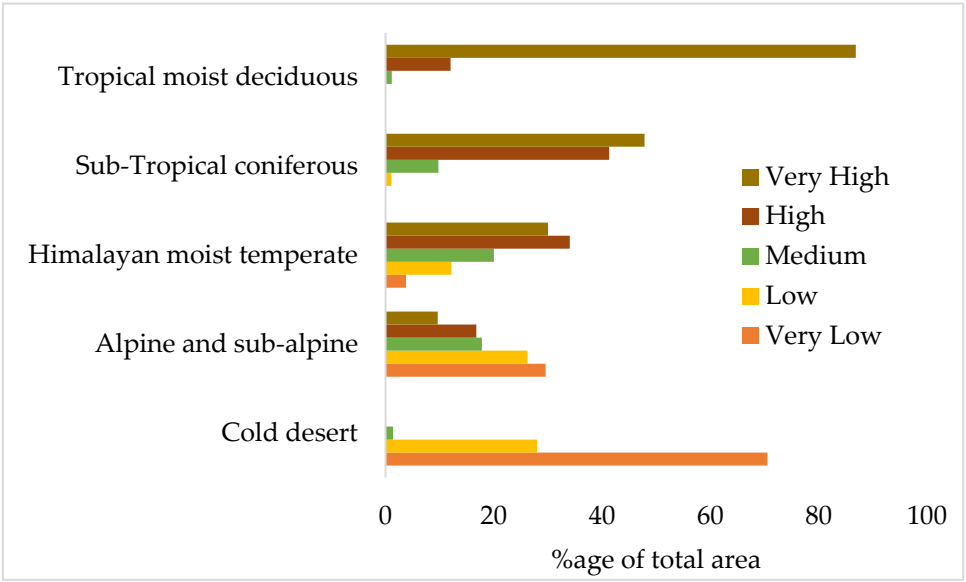

Figure 9. Percentage of area of each forest type under the varying intensities of FFS.

3.5. District-Wise Analysis of FFS

There are 47 districts altogether in Uttarakhand (UK), Himachal Pradesh (HP), and Jammu and Kashmir (JK). By analyzing the percentage of the area of each district (Figure 10 and Table 10) that fell in each of the five distinct FFS zones, it was found that the very high FFS zone covered 17 districts out of the total of 47 districts. These included Haridwar, Nainital, and Udham Singh Nagar (UK); Sirmaur, Bilaspur, Hamirpur, Kangra, Mandi, Solan, and Una (HP); and Baramulla, Kathua, Badgam, Pulwama, Shupiyan, Samba, and Jammu (JK). Udham Singh Nagar, with 86.25% of its total area in the very high FFS zone, was the most vulnerable district of the IWH region. The districts falling under the high FFS zone included Almora, Bageshwar, Champawat, Dehradun, Pauri Garhwal, and Tehri Garhwal, (UK); Shimla (HP); and Mirpur, Poonch, Udhampur, Kupwara, Rajauri, Raisi, Srinagar, Doda, and Ramban (JK). Srinagar led the pack with 58.60% of its whole area falling in the high FFS zone. None of the districts fell under a medium FFS zone. It was found that seven districts fell under the very low FFS zone. These included Chamoli, Pithoragarh, and Uttarkashi (UK); Chamba, Kullu, Lahul and Spiti (HP); and Kishtwar (JK). Among these, Lahul and Spiti had 63.87% of its total area under this category, making it the district least vulnerable to forest fire. Seven districts fell under the low FFS zone, namely, Rudraprayag (UK); Kinnaur (HP); and Muzzafarabad, Anantnag, Bandipura, Ganderbal, and Kulgam (JK). Comparing all of them, Bandipura had the maximum % (52.93%) of its area under this category.

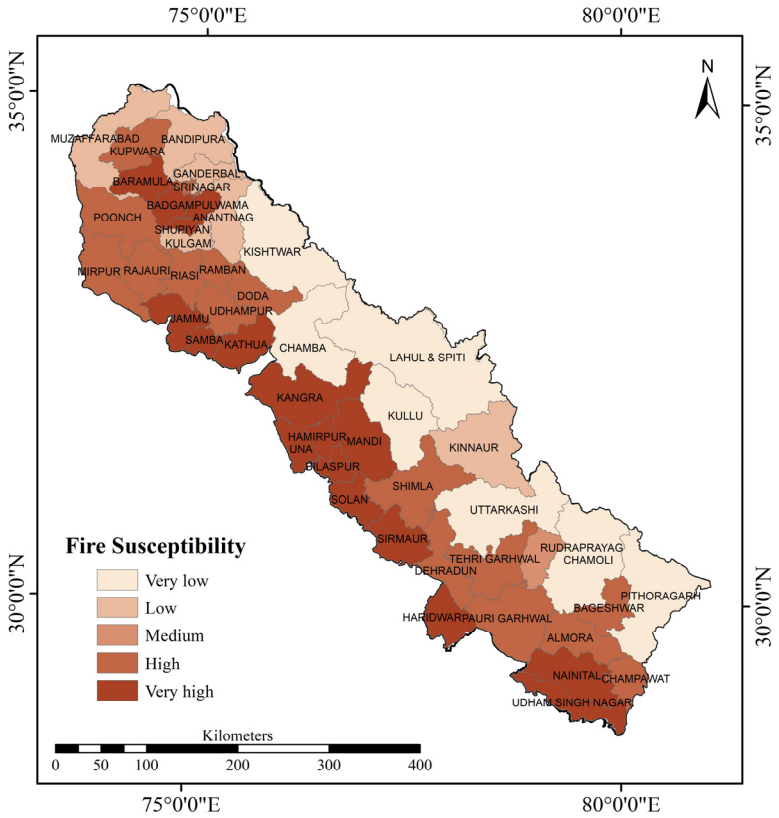

Figure 10. District-wise forest fire susceptibility in the IWH region.

Table 10. District-wise analysis (area and percentage) of FFS intensity.

District	VL_Area (sq·km)	Area_%	L_Area (sq·km)	Area_%	M_Area (sq·km)	Area_%	H_Area (sq·km)	Area_%	VH_Area (sq·km)	Area_%	Total Area (sq·km)
ALMORA	0.00	**0.00**	124.00	**2.98**	1000.00	**24.04**	1740.00	**41.84**	1295.00	**31.14**	**4159**
BAGESHWAR	475.00	**15.97**	322.00	**10.83**	767.00	**25.79**	909.00	**30.56**	501.00	**16.85**	**2974**
BILASPUR	0.00	**0.00**	7.00	**0.46**	138.00	**9.04**	566.00	**37.09**	815.00	**53.41**	**1526**
CHAMBA	3083.00	**33.92**	2088.00	**22.97**	1840.00	**20.24**	1374.00	**15.12**	705.00	**7.76**	**9090**
CHAMPAWAT	0.00	**0.00**	67.00	**2.99**	485.00	**21.64**	974.00	**43.46**	715.00	**31.91**	**2241**
DEHRADUN	0.00	**0.00**	222.00	**5.44**	861.00	**21.10**	1731.00	**42.43**	1266.00	**31.03**	**4080**
HAMIRPUR	0.00	**0.00**	0.00	**0.00**	27.00	**1.75**	473.00	**30.71**	1040.00	**67.53**	**1540**
HARIDWAR	0.00	**0.00**	5.00	**0.17**	104.00	**3.64**	824.00	**28.83**	1925.00	**67.35**	**2858**
KANGRA	430.00	**5.51**	980.00	**12.56**	570.00	**7.30**	1631.00	**20.90**	4194.00	**53.73**	**7805**
KULLU	2121.00	**27.92**	1631.00	**21.47**	1891.00	**24.89**	1469.00	**19.33**	486.00	**6.40**	**7598**
MANDI	0.00	**0.00**	141.00	**2.59**	831.00	**15.28**	2157.00	**39.67**	2308.00	**42.45**	**5437**
NAINITAL	0.00	**0.00**	67.00	**1.28**	585.00	**11.17**	2142.00	**40.89**	2445.00	**46.67**	**5239**
PAURI GARHWAL	0.00	**0.00**	265.00	**3.85**	1903.00	**27.63**	3328.00	**48.32**	1391.00	**20.20**	**6887**
RUDRAPRAYAG	371.00	**13.85**	485.00	**18.11**	897.00	**33.50**	731.00	**27.30**	194.00	**7.24**	**2678**
SHIMLA	182.00	**2.60**	607.00	**8.68**	1400.00	**20.01**	2783.00	**39.79**	2023.00	**28.92**	**6995**
SIRMAUR	0.00	**0.00**	77.00	**2.10**	860.00	**23.50**	1194.00	**32.63**	1528.00	**41.76**	**3659**
SOLAN	0.00	**0.00**	3.00	**0.12**	81.00	**3.18**	928.00	**36.44**	1535.00	**60.27**	**2547**
TEHRI GARHWAL	299.00	**5.69**	271.00	**5.16**	1450.00	**27.60**	2208.00	**42.03**	1026.00	**19.53**	**5254**
UDHAM SINGH NAGAR	0.00	**0.00**	0.00	**0.00**	30.00	**0.96**	401.00	**12.80**	2703.00	**86.25**	**3134**
UNA	0.00	**0.00**	2.00	**0.10**	31.00	**1.58**	528.00	**26.91**	1401.00	**71.41**	**1962**
MIRPUR	0.00	**0.00**	68.00	**1.41**	598.00	**12.38**	2351.00	**48.65**	1815.00	**37.56**	**4832**
MUZAFFARABAD	798.00	**11.99**	1745.00	**26.22**	1721.00	**25.86**	1734.00	**26.06**	657.00	**9.87**	**6655**

Table 10. *Cont.*

District	VL_Area (sq·km)	Area_%	L_Area (sq·km)	Area_%	M_Area (sq·km)	Area_%	H_Area (sq·km)	Area_%	VH_Area (sq·km)	Area_%	Total Area (sq·km)
POONCH	10.00	**0.16**	284.00	**4.67**	686.00	**11.27**	3391.00	**55.72**	1715.00	**28.18**	**6086**
ANANTNAG	147.00	**3.73**	1143.00	**28.97**	606.00	**15.36**	1099.00	**27.85**	951.00	**24.10**	**3946**
BARAMULA	1.00	**0.03**	228.00	**7.59**	400.00	**13.32**	1186.00	**39.49**	1188.00	**39.56**	**3003**
KATHUA	4.00	**0.12**	153.00	**4.54**	624.00	**18.52**	1033.00	**30.65**	1556.00	**46.17**	**3370**
UDHAMPUR	3.00	**0.09**	60.00	**1.86**	478.00	**14.84**	1441.00	**44.75**	1238.00	**38.45**	**3220**
BADGAM	3.00	**0.17**	393.00	**21.66**	137.00	**7.55**	603.00	**33.24**	678.00	**37.38**	**1814**
BANDIPURA	320.00	**5.58**	3035.00	**52.93**	1296.00	**22.60**	725.00	**12.64**	358.00	**6.24**	**5734**
GANDERBAL	75.00	**3.16**	789.00	**33.25**	627.00	**26.42**	586.00	**24.69**	296.00	**12.47**	**2373**
KULGAM	82.00	**4.48**	605.00	**33.08**	249.00	**13.61**	406.00	**22.20**	487.00	**26.63**	**1829**
KUPWARA	0.00	**0.00**	534.00	**13.19**	1002.00	**24.76**	1312.00	**32.42**	1199.00	**29.63**	**4047**
PULWAMA	0.00	**0.00**	73.00	**5.58**	130.00	**9.94**	470.00	**35.93**	635.00	**48.55**	**1308**
RAJAURI	0.00	**0.00**	94.00	**2.50**	501.00	**13.32**	1726.00	**45.88**	1441.00	**38.30**	**3762**
RAMBAN	0.00	**0.00**	230.00	**12.52**	670.00	**36.47**	683.00	**37.18**	254.00	**13.83**	**1837**
RIASI	42.00	**1.52**	416.00	**15.07**	787.00	**28.50**	885.00	**32.05**	631.00	**22.85**	**2761**
SHUPIYAN	7.00	**0.97**	39.00	**5.38**	25.00	**3.45**	277.00	**38.21**	377.00	**52.00**	**725**
SRINAGAR	0.00	**0.00**	0.00	**0.00**	20.00	**4.99**	235.00	**58.60**	146.00	**36.41**	**401**
KISHTWAR	5448.00	**47.28**	2996.00	**26.00**	1891.00	**16.41**	954.00	**8.28**	235.00	**2.04**	**11,524**
DODA	186.00	**5.43**	240.00	**7.00**	988.00	**28.82**	1329.00	**38.77**	685.00	**19.98**	**3428**
SAMBA	0.00	**0.00**	0.00	**0.00**	111.00	**8.80**	321.00	**25.44**	830.00	**65.77**	**1262**
CHAMOLI	3270.00	**31.52**	2916.00	**28.11**	2342.00	**22.57**	1555.00	**14.99**	292.00	**2.81**	**10,375**
KINNAUR	2829.00	**32.35**	4129.00	**47.22**	1174.00	**13.42**	511.00	**5.84**	102.00	**1.17**	**8745**
LAHUL AND SPITI	12,161.00	**63.87**	6221.00	**32.68**	583.00	**3.06**	71.00	**0.37**	3.00	**0.02**	**19,039**
PITHORAGARH	3096.00	**33.69**	2367.00	**25.76**	1589.00	**17.29**	1323.00	**14.40**	815.00	**8.87**	**9190**
UTTARKASHI	3115.00	**29.17**	2769.00	**25.93**	2180.00	**20.41**	1978.00	**18.52**	637.00	**5.96**	**10,679**
JAMMU	0.00	**0.00**	9.00	**0.28**	190.00	**5.82**	1167.00	**35.73**	1900.00	**58.18**	**3266**

4. Discussion

The mapping and evaluation of FFS hold significant importance in the contexts of disaster management and the sustainable development of forests. Once the appropriate indicators have been identified, it becomes straightforward to assess the level of susceptibility for each setting. The vulnerability assessment for the Indian Western Himalayas (IWH) region, encompassing the states of Jammu and Kashmir, Himachal Pradesh, and Uttarakhand, was conducted by employing remote sensing data and the GIS-based Fuzzy-AHP technique. Remote sensing data and GIS-based analysis offer the advantage of being able to monitor large areas from a distance, providing valuable information on the state of forests and potential threats such as forest fires [86]. The Fuzzy-AHP technique is an effective tool in multi-criteria evaluations and has been found effective for vulnerability assessment in various studies, including [87–90]. In this investigation, a Fuzzy-AHP model was created and evaluated for assessing vulnerability to forest fires. The results demonstrated that the model exhibits substantial efficacy in this area as well.

This study found that the forest fire vulnerability of the IWH region is mainly controlled by the forest type, temperature, and distance to settlement. This is in line with previous research, including [91,92], that has shown similar factors to have a significant influence on forest fire susceptibility. By superimposing the forest type map of the IWH region onto the FFS zones map, we were able to obtain a comprehensive analysis of forest fires in our research area based on the different forest types. Since the forest type is influenced by rainfall and temperature, which are regulated by the elevation in the mountainous terrain, it is necessary to acknowledge that elevation is the hidden controller of forest fire vulnerability in the IWH region. This is consistent with the dispersion of the relatively small number of forest fire emission patches in the higher elevations of the IWH [93]. Moreover, regions at higher elevations have lower temperatures, leading to limited vegetation. Conversely, as elevation decreases, temperatures become more favorable, and as a result, the lower elevations in the Himalayas have a dense forest canopy, making these areas particularly susceptible to the risks associated with forest fires. This pattern is effectively conveyed through what was discovered in this research work.

The cold desert lies at an elevation of over 4000 m in the study region and has 70.51% of its area in the very low FFS zone. Alpine and subalpine forests lie within the elevation range of 1000–7000 m and are mainly dominated by the very low FFS zone. The Himalayan moist temperate forest is situated at elevations ranging from 1000 to 4000 m, and approximately 34% of its total area falls in the high FFS zone. In comparison, the subtropical coniferous forest, located within the elevation range of 1000 to 2000 m, has 47.84% of its area classified as in the very high FFS zone. Lastly, the tropical moist deciduous forest, found at elevations below 1000 m, exhibited the highest vulnerability among the forest types in the IWH region, with approximately 86.85% of its area falling in the very high FFS zone.

The present study's results can be effectively matched with the research conducted by [17], which examined the spatial pattern and trends of forest fires in active fire data derived from a moderate-resolution imaging spectroradiometer and spanning the years 2001 to 2020. That study revealed that the evergreen needle-leaf forests (resembling subtropical coniferous forests in terms of the same flora species found, i.e., *Pinus roxburghii* (Chir pine)) experienced the most intense forest fires (57.07%), followed by deciduous broadleaf forests with 24.44%, shrubland (resembling alpine and subalpine forests) with 8.9%, evergreen broadleaf forests (resembling tropical moist deciduous forests) with 4.47%, mixed forests with 4.15%, and grassland with 0.9% of fire intensity. The role of elevation in [13] also indicated the highest likelihood (>0.8) of fire at elevations < 2500 m, and a reduced probability of fire at higher-elevation regions. They looked at the predicted fire susceptibility for 2030, 2040, and 2050, along with the change in elevation.

According to [20], a forest fire in 2016 had a significant impact on the land area in Himachal Pradesh, affecting over 45 km^2. Similarly, Uttarakhand saw a substantial impact, with around 31.85 km^2 being affected by the same forest fire event. The larger affected portion of the forest had an abundance of Chir pine. Chir pine, being among the major flora

species found in subtropical coniferous forests in the Himalayas, makes this forest highly vulnerable to fire. In our study, the subtropical coniferous forest had 47.8% of its area under the very high FFS zone, which included the Kathua, Jammu, and Samba districts of JK, the Kangra and Una districts of HP, and the Nainital and Haridwar districts of UK. A district-wise analysis in our study clearly indicated that districts at lower elevations and with higher levels of anthropogenic activities fell under the very high FFS zone. Pithoragarh, Chamoli, Lahul and Spiti, Kullu, Kishtwar, and Uttarkashi are in the elevation range of >4000 m and they were the least vulnerable to forest fire, whereas the Una, Baramulla, Kathua, Badgam, Pulwama, Shupiyan, Samba, and Jammu districts of JK, Bilaspur, Hamirpur, Kangra, Mandi, Solan, and Sirmaur districts of Himachal Pradesh, and Haridwar, Nainital, and Udham Singh Nagar districts of Uttarakhand, which lie within the elevation range of 1000–2000 m, were the most susceptible districts in the IWH states. While [94] revealed that the Sirmaur district falls under the very-high- to high-risk zones, our study placed 36.81% of its area under the very-high- to high-risk zones.

Based on this assessment using a few selected vulnerability indicators, it was found that the forests at higher elevations, such as the cold desert and alpine forests (dry, moist, and subalpine), are the least vulnerable forests compared to the other forest-type groups of the IWH in the current scenario. However, there are not many studies that specifically show how vulnerable particular districts are at different elevations in the IWH region to forest fires.

Despite the impressive performance by this study's model, it is important to note that its limitations lie in the dependence on decision makers' assumptions and approximations. Moreover, there are the inherent challenges of uncertainty and subjectivity when defining preferences using fuzzy numbers. In addition, the scope of this research was limited to the IWH region. Thus, it should be noted that these findings may not possess direct applicability to other geographical regions.

5. Conclusions

One of the most notable signs of the destruction of the world's forest systems is forest fires. The objective of this assessment was to determine the spatial vulnerability to forest fire in the IWH region, which is regularly subject to forest fire events. A forest fire susceptibility map was created using a flexible and efficient strategy that combined remote sensing, GIS, and the Fuzzy-AHP technique. The map was created at two different levels, with one being the determination of susceptibility individually according to physiography, meteorology, or anthropogenic influence in the IWH region, followed by the combination of these three into a comprehensive FFS map. The conclusions of this study are as follows:

- The IWH region has significant susceptibility to forest fire as nearly 50% area of the region is characterized as a high or very high FFS zone.
- The incidence of forest fire is specific to the forest types in the IWH region. The higher susceptibility is associated with the subtropical coniferous forests and tropical moist deciduous forests owing to the dominance of the relatively more flammable Chir pine species, in addition to the higher FCR.
- The forest fire incidence is regulated majorly by elevation, temperature, and moisture conditions in the region, and by nearness to the settlements and the roads in the IWH region.

The results of this research will enhance the ability of forest planners and managers to provide improved forest protection and preventive services within the designated study region. According to several studies and publications, a decreased level of human intervention can play a significant role in preserving forest ecosystems. It is recommended that the government establish stringent laws and regulations to effectively mitigate human disruptions to the environment, with the aim of conserving and promoting the nation's diversified and significant physiography.

Author Contributions: Conceptualization, M.K.; methodology, A.T.; software, S.I.M.; investigation, S.B.; validation, N.S.; data curation, P., A.T. and S.I.M.; resources, M.K., N.S., N.K.V. and D.K.T.; formal analysis, P., M.K., A.T., S.I.M. and S.B.; writing—original draft preparation, P., A.T., S.B., S.I.M. and M.K.; writing—review and editing, P., A.T., S.I.M., S.B., R.A. and M.K.; visualization, N.S.; supervision, N.S. and M.K.; project administration, M.K., N.K.V. and D.K.T.; funding acquisition, R.A. All authors have read and agreed to the published version of the manuscript.

Funding: This research was partially funded by Grant-in-Aid for Scientific Research (c), grant number 21K05664.

Data Availability Statement: All data generated or analyzed during the study are included in this published article.

Acknowledgments: The authors express their gratitude to the Department of Geography at the Central University of Haryana, Mahendragarh, India, for providing a technically robust platform, supporting software services (ArcGIS 10.7 and SPSS 26.0), and a supportive atmosphere for the successful execution of this research.

Conflicts of Interest: The authors unanimously declare that there are no conflict of interest to declares.

References

1. Gheshlaghi, H.A.; Feizizadeh, B.; Blaschke, T. GIS-based forest fire risk mapping using the analytical network process and fuzzy logic. *J. Environ. Plan. Manag.* **2019**, *63*, 481–499. [CrossRef]
2. Mafi-Gholami, D.; Jaafari, A.; Zenner, E.K.; Kamari, A.N.; Bui, D.T. Spatial modeling of exposure of mangrove ecosystems to multiple environmental hazards. *Sci. Total Environ.* **2020**, *740*, 140167. [CrossRef] [PubMed]
3. Nuthammachot, N.; Stratoulias, D. A GIS- and AHP-based approach to map fire risk: A case study of Kuan Kreng peat swamp forest, Thailand. *Geocarto Int.* **2019**, *36*, 212–225. [CrossRef]
4. Tuyen, T.T.; Jaafari, A.; Yen, H.P.H.; Nguyen-Thoi, T.; Van Phong, T.; Nguyen, H.D.; Van Le, H.; Phuong, T.T.M.; Nguyen, S.H.; Prakash, I.; et al. Mapping forest fire susceptibility using spatially explicit ensemble models based on the locally weighted learning algorithm. *Ecol. Inform.* **2021**, *63*, 101292. [CrossRef]
5. Giglio, L.; Boschetti, L.; Roy, D.P.; Humber, M.L.; Justice, C.O. The Collection 6 MODIS burned area mapping algorithm and product. *Remote Sens. Environ.* **2018**, *217*, 72–85. [CrossRef]
6. Jaafari, A.; Mafi-Gholami, D.; Pham, B.T.; Tien Bui, D. Wildfire Probability Mapping: Bivariate vs. Multivariate Statistics. *Remote Sens.* **2019**, *11*, 618. [CrossRef]
7. Ridder, R.M. Global forest resources assessment 2010: Options and recommendations for a global remote sensing survey of forests. In *Global Remote Sensing Survey of Forests*; FAO: Rome, Italy, 2007; Volume 141.
8. Jain, P.; Coogan, S.C.P.; Subramanian, S.G.; Crowley, M.; Taylor, S.W.; Flannigan, M.D. A review of machine learning applications in wildfire science and management. *Environ. Rev.* **2020**, *28*, 478–505. [CrossRef]
9. Tariq, A.; Shu, H.; Siddiqui, S.; Mousa, B.G.; Munir, I.; Nasri, A.; Waqas, H.; Lu, L.; Baqa, M.F. Forest fire monitoring using spatial-statistical and Geo-spatial analysis of factors determining forest fire in Margalla Hills, Islamabad, Pakistan. *Geomat. Nat. Hazards Risk* **2021**, *12*, 1212–1233. [CrossRef]
10. Hansen, M.C.; Potapov, P.V.; Moore, R.; Hancher, M.; Turubanova, S.A.; Tyukavina, A.; Thau, D.; Stehman, S.V.; Goetz, S.J.; Loveland, T.R.; et al. High-resolution global maps of 21st-century forest cover change. *Science* **2013**, *342*, 850–853. [CrossRef]
11. Reddy, C.S.; Bird, N.G.; Sreelakshmi, S.; Manikandan, T.M.; Asra, M.; Krishna, P.H.; Jha, C.S.; Rao, P.V.N.; Diwakar, P.G. Identification and characterization of spatio-temporal hotspots of forest fires in South Asia. *Environ. Monit. Assess.* **2019**, *191*, 1–17. [CrossRef]
12. Mohanty, A.; Vidur, M. *Managing Forest Fires in a Changing Climate*; Council on Energy, Environment and Water: New Delhi, India, 2022.
13. Bar, S.; Parida, B.R.; Pandey, A.C.; Shankar, B.U.; Kumar, P.; Panda, S.K.; Behera, M.D. Modeling and prediction of fire occurrences along an elevational gradient in Western Himalayas. *Appl. Geogr.* **2023**, *151*, 102867. [CrossRef]
14. Srivastava, P.; Garg, A. Forest Fires in India: Regional and Temporal Analyses. *J. Trop. For. Sci.* **2013**, *25*, 228–239.
15. Vadrevu, K.P.; Lasko, K.; Giglio, L.; Schroeder, W.; Biswas, S.; Justice, C. Trends in Vegetation fires in South and Southeast Asian Countries. *Sci. Rep.* **2019**, *9*, 7422. [CrossRef] [PubMed]
16. Kumar, S.; Chaudhary, C.; Biswas, T.; Ghosh, S.; Ashutosh, S. *Identification of Fire Prone Forest Areas Based on GIS Analysis of Archived Forest Fire Points Detected in Last Thirteen Years*; Ministry of Environment, Forest & Climate Change, Government of India: Dehradun, India, 2019; Volume 1.
17. Kumar, M. Forestry Policies and Practices to Promote Climate Change Adaptation in the Indian Western Himalayan States. In *Climate Change Adaptation, Risk Management and Sustainable Practices in the Himalaya*; Sharma, S., Kuniyal, J.C., Chand, P., Singh, P., Eds.; Springer International Publishing: Cham, Switzerland, 2023; pp. 65–87. [CrossRef]
18. Chakraborty, A.; Joshi, P. Mapping disaster vulnerability in India using analytical hierarchy process. *Geomat. Nat. Hazards Risk* **2014**, *7*, 308–325. [CrossRef]

19. Babu, K.V.S.; Roy, A.; Prasad, P.R. Forest fire risk modeling in Uttarakhand Himalaya using TERRA satellite datasets. *Eur. J. Remote Sens.* **2016**, *49*, 381–395. [CrossRef]
20. Bhattarai, N.; Dahal, S.; Thapa, S.; Pradhananga, S.; Karky, B.S.; Rawat, R.S.; Windhorst, K.; Watanabe, T.; Thapa, R.B.; Avtar, R. Forest fire in the hindu kush Himalayas: A major challenge for climate action. *J. For. Livelihood* **2022**, *21*, 14–31. [CrossRef]
21. Bar, S.; Parida, B.R.; Roberts, G.; Pandey, A.C.; Acharya, P.; Dash, J. Spatio-temporal characterization of landscape fire in relation to anthropogenic activity and climatic variability over the Western Himalaya, India. *GIScience Remote Sens.* **2021**, *58*, 281–299. [CrossRef]
22. Tian, X.; Zhao, F.; Shu, L.; Wang, M. Distribution characteristics and the influence factors of forest fires in China. *For. Ecol. Manag.* **2013**, *310*, 460–467. [CrossRef]
23. Key, C.; Benson, N. Landscape assessment: Remote sensing of severity, the normalized burn ratio and ground measure of severity, the composite burn index. In *Fire Effects Monitoring and Inventory System*; USDA Forest Service, Rocky Mountain Research Station: Ogden, UT, USA, 2005.
24. Wang, J.; Rich, P.M.; Price, K.P.; Kettle, W.D. Relations between NDVI and tree productivity in the central Great Plains. *Int. J. Remote Sens.* **2004**, *25*, 3127–3138. [CrossRef]
25. Justice, C.; Townshend, J.; Vermote, E.; Masuoka, E.; Wolfe, R.; Saleous, N.; Roy, D.; Morisette, J. An overview of MODIS Land data processing and product status. *Remote Sens. Environ.* **2002**, *83*, 3–15. [CrossRef]
26. Polychronaki, A.; Gitas, I.Z.; Veraverbeke, S.; Debien, A. Evaluation of ALOS PALSAR Imagery for Burned Area Mapping in Greece Using Object-Based Classification. *Remote Sens.* **2013**, *5*, 5680–5701. [CrossRef]
27. Hong, H.; Naghibi, S.A.; Dashtpagerdi, M.M.; Pourghasemi, H.R.; Chen, W. A comparative assessment between linear and quadratic discriminant analyses (LDA-QDA) with frequency ratio and weights-of-evidence models for forest fire susceptibility mapping in China. *Arab. J. Geosci.* **2017**, *10*, 167. [CrossRef]
28. Milanović, S.; Marković, N.; Pamučar, D.; Gigović, L.; Kostić, P.; Milanović, S.D. Forest Fire Probability Mapping in Eastern Serbia: Logistic Regression versus Random Forest Method. *Forests* **2020**, *12*, 5. [CrossRef]
29. Iban, M.C.; Sekertekin, A. Machine learning based wildfire susceptibility mapping using remotely sensed fire data and GIS: A case study of Adana and Mersin provinces, Turkey. *Ecol. Inform.* **2022**, *69*, 101647. [CrossRef]
30. Babu, K.N.; Gour, R.; Ayushi, K.; Ayyappan, N.; Parthasarathy, N. Environmental drivers and spatial prediction of forest fires in the Western Ghats biodiversity hotspot, India: An ensemble machine learning approach. *For. Ecol. Manag.* **2023**, *540*, 121057. [CrossRef]
31. Abujayyab, S.K.M.; Kassem, M.M.; Khan, A.A.; Wazirali, R.; Coşkun, M.; Taşoğlu, E.; Öztürk, A.; Toprak, F. Wildfire Susceptibility Mapping Using Five Boosting Machine Learning Algorithms: The Case Study of the Mediterranean Region of Turkey. *Adv. Civ. Eng.* **2022**, *2022*, 3959150. [CrossRef]
32. Mohajane, M.; Costache, R.; Karimi, F.; Pham, Q.B.; Essahlaoui, A.; Nguyen, H.; Laneve, G.; Oudija, F. Application of remote sensing and machine learning algorithms for forest fire mapping in a Mediterranean area. *Ecol. Indic.* **2021**, *129*, 107869. [CrossRef]
33. Oh, H.-J.; Syifa, M.; Lee, C.-W.; Lee, S. Land Subsidence Susceptibility Mapping Using Bayesian, Functional, and Meta-Ensemble Machine Learning Models. *Appl. Sci.* **2019**, *9*, 1248. [CrossRef]
34. Jha, M.K.; Chowdary, V.M.; Chowdhury, A. Groundwater assessment in Salboni Block, West Bengal (India) using remote sensing, geographical information system and multi-criteria decision analysis techniques. *Hydrogeol. J.* **2010**, *18*, 1713–1728. [CrossRef]
35. Pietersen, K. Multiple criteria decision analysis (MCDA): A tool to support sustainable management of groundwater resources in South Africa. *Water SA* **2007**, *32*, 119–128. [CrossRef]
36. Saaty, T.L. *The Analytic Hierarchy Process*; McGraw-Hill: New York, NY, USA, 1980.
37. Das, B.; Pal, S.C. Combination of GIS and fuzzy-AHP for delineating groundwater recharge potential zones in the critical Goghat-II block of West Bengal, India. *HydroResearch* **2019**, *2*, 21–30. [CrossRef]
38. Kahraman, C.; Ruan, D.; Doğan, I. Fuzzy group decision-making for facility location selection. *Inf. Sci.* **2003**, *157*, 135–153. [CrossRef]
39. Saaty, T.L.; Tran, L.T. On the invalidity of fuzzifying numerical judgments in the Analytic Hierarchy Process. *Math. Comput. Model.* **2007**, *46*, 962–975. [CrossRef]
40. van Laarhoven, P.; Pedrycz, W. A fuzzy extension of Saaty's priority theory. *Fuzzy Sets Syst.* **1983**, *11*, 229–241. [CrossRef]
41. Eskandari, S. A new approach for forest fire risk modeling using fuzzy AHP and GIS in Hyrcanian forests of Iran. *Arab. J. Geosci.* **2017**, *10*, 190. [CrossRef]
42. Güngöroğlu, C. Determination of forest fire risk with fuzzy analytic hierarchy process and its mapping with the application of GIS: The case of Turkey/Çakırlar. *Hum. Ecol. Risk Assess. Int. J.* **2016**, *23*, 388–406. [CrossRef]
43. Tiwari, A.; Shoab, M.; Dixit, A. GIS-based forest fire susceptibility modeling in Pauri Garhwal, India: A comparative assessment of frequency ratio, analytic hierarchy process and fuzzy modeling techniques. *Nat. Hazards* **2020**, *105*, 1189–1230. [CrossRef]
44. Chaudhry, A.K.; Kumar, K.; Alam, M.A. Mapping of groundwater potential zones using the fuzzy analytic hierarchy process and geospatial technique. *Geocarto Int.* **2019**, *36*, 2323–2344. [CrossRef]
45. Padma, S.; Sanjeevi, S. Jeffries Matusita based mixed-measure for improved spectral matching in hyperspectral image analysis. *Int. J. Appl. Earth Obs. Geoinf.* **2014**, *32*, 138–151. [CrossRef]
46. Barry, R.G. Mountain Weather and Climate. In *Mountain Weather and Climate*; Routledge: Oxfordshire, UK, 2008. Available online: https://www.cabdirect.org/cabdirect/abstract/20093032476 (accessed on 19 August 2023).

47. Harlow, R.C.; Burke, E.J.; Scott, R.L.; Shuttleworth, W.J.; Brown, C.M.; Petti, J.R. Research Note: Derivation of temperature lapse rates in semi-arid south-eastern Arizona. *Hydrol. Earth Syst. Sci.* **2004**, *8*, 1179–1185. [CrossRef]
48. Minder, J.R.; Mote, P.W.; Lundquist, J.D. Surface temperature lapse rates over complex terrain: Lessons from the Cascade Mountains. *J. Geophys. Res. Atmos.* **2010**, *115*. [CrossRef]
49. Finney, M.A.; McHugh, C.W.; Grenfell, I.C.; Riley, K.L.; Short, K.C. A simulation of probabilistic wildfire risk components for the continental United States. *Stoch. Environ. Res. Risk Assess.* **2011**, *25*, 973–1000. [CrossRef]
50. Andrews, P.L. *BEHAVE: Fire Behavior Prediction and Fuel Modeling System: BURN Subsystem, Part 1*; U.S. Department of Agriculture, Forest Service, Intermountain Research Station: Washington, DC, USA, 1986.
51. Bhusal, S.; Mandal, R.A. Forest fire occurrence, distribution and future risks in Arghakhanchi district, Nepal. *Int. J. Geogr. Geol. Environ.* **2020**, *2*, 10–20.
52. Minár, J.; Evans, I.S.; Jenčo, M. A comprehensive system of definitions of land surface (topographic) curvatures, with implications for their application in geoscience modelling and prediction. *Earth-Sci. Rev.* **2020**, *211*, 103414. [CrossRef]
53. Kimerling, A.J.; Muehrcke, P.C.; Muehrcke, J.O.; Muehrcke, P. *Map Use: Reading, Analysis, Interpretation*; ESRI Press Academic: Redlands, CA, USA, 2016.
54. Riley, S.J. A Terrain Ruggedness Index that Quantifies Topographic Heterogeneity. 1999. Available online: https://download.osgeo.org/qgis/doc/reference-docs/Terrain_Ruggedness_Index.pdf (accessed on 19 August 2023).
55. Jensen, J.R. *Remote Sensing of the Environment: An Earth Resource Perspective 2/e*; Pearson Education India: Bengaluru, India, 2009.
56. Rouse, J.W.; Haas, R.H.; Deering, D.W.; Schell, J.A.; Harlan, J.C. Monitoring the Vernal Advancement and Retrogradation (Green Wave Effect) of Natural Vegetation. E75-10354, Nov. 1974. Available online: https://ntrs.nasa.gov/citations/19750020419 (accessed on 19 August 2023).
57. Tucker, C.J. Red and photographic infrared linear combinations for monitoring vegetation. *Remote Sens. Environ.* **1979**, *8*, 127–150. [CrossRef]
58. Cohen, J. Preventing disaster: Home ignitability in the wildland-urban interface. *J. For.* **2000**, *98*, 15–21. [CrossRef]
59. Pyne, S.J. Wild Hearth A Prolegomenon to the Cultural Fire History of Northern Eurasia. In *Fire in Ecosystems of Boreal Eurasia*; Goldammer, J.G., Furyaev, V.V., Eds.; Forestry Sciences; Springer: Dordrecht, The Netherlands, 1996; pp. 21–44. [CrossRef]
60. Rothermel, R.C. *A Mathematical Model for Predicting Fire Spread in Wildland Fuels. Intermountain Forest & Range Experiment Station, Forest Service*; U.S. Department of Agriculture: Washington, DC, USA, 1972.
61. Karki, S.; Pforte, B.; Karky, B.S.; Statz, J.; Dangi, R.B.; Khanal, D.R.; Windhorst, K. The development of REDD+ safeguards in the Hindu Kush Himalaya: Recent experiences and processes. *ICIMOD Work. Pap.* **2017**. Available online: https://www.cabdirect.org/cabdirect/abstract/20183165027 (accessed on 19 August 2023).
62. Thakur, S.; Dhyani, R.; Negi, V.S.; Patley, M.; Rawal, R.; Bhatt, I.; Yadava, A. Spatial forest vulnerability profile of major forest types in Indian Western Himalaya. *For. Ecol. Manag.* **2021**, *497*, 119527. [CrossRef]
63. Mandel, J.; Amram, S.; Beezley, J.D.; Kelman, G.; Kochanski, A.K.; Kondratenko, V.Y.; Vejmelka, M. Recent advances and applications of WRF–SFIRE. *Nat. Hazards Earth Syst. Sci.* **2014**, *14*, 2829–2845. [CrossRef]
64. Negi, M.; Kumar, A. Assessment of increasing threat of forest fires in Uttarakhand, using remote sensing and GIS techniques. *Glob. J. Adv. Res.* **2016**, *3*, 457–468.
65. Pimont, F.; Dupuy, J.-L.; Linn, R.R. Coupled slope and wind effects on fire spread with influences of fire size: A numerical study using FIRETEC. *Int. J. Wildland Fire* **2012**, *21*, 828–842. [CrossRef]
66. E Calkin, D.; Thompson, M.P.; A Finney, M. Negative consequences of positive feedbacks in US wildfire management. *For. Ecosyst.* **2015**, *2*, 9. [CrossRef]
67. Oreski, D. Strategy development by using SWOT—AHP. *Tem J.* **2012**, *1*, 4.
68. Dey, P.K. Project risk management using multiple criteria decision-making technique and decision tree analysis: A case study of Indian oil refinery. *Prod. Plan. Control.* **2011**, *23*, 903–921. [CrossRef]
69. Çoban, H.; Erdin, C. Forest fire risk assessment using GIS and AHP integration in Bucak forest enterprise, Turkey. *Appl. Ecol. Environ. Res.* **2020**, *18*, 1567–1583. [CrossRef]
70. Fazlollahtabar, H.; Eslami, H.; Salmani, H. Designing a Fuzzy Expert System to Evaluate Alternatives in Fuzzy Analytic Hierarchy Process. *J. Softw. Eng. Appl.* **2010**, *3*, 409–418. [CrossRef]
71. Mohammadi, F.; Shabanian, N.; Pourhashemi, M.; Fatehi, P. Risk zone mapping of forest fire using GIS and AHP in a part of Paveh forests. *Iran. J. For. Poplar Res.* **2010**, *18*, 569–586. [CrossRef]
72. Buckley, J.J. Fuzzy hierarchical analysis. *Fuzzy Sets Syst.* **1985**, *17*, 233–247. [CrossRef]
73. Chang, D.-Y. Applications of the extent analysis method on fuzzy AHP. *Eur. J. Oper. Res.* **1996**, *95*, 649–655. [CrossRef]
74. Zadeh, L.A. Fuzzy sets. *Inf. Control* **1965**, *8*, 338–353. [CrossRef]
75. Esmaeili, A.; Kahnali, R.A.; Rostamzadeh, R.; Kazimieras, E.; Sepahvand, A. The formulation of organizational strategies through integration of freeman model, SWOT, and fuzzy MCDM methods: A case study of oil industry. *Transform. Bus. Econ.* **2014**, *13*, 602–627.
76. Chen, H.; Wood; Linstead, C.; Maltby, E. Uncertainty analysis in a GIS-based multi-criteria analysis tool for river catchment management. *Environ. Model. Softw.* **2011**, *26*, 395–405. [CrossRef]

77. Kannan, D.; Khodaverdi, R.; Olfat, L.; Jafarian, A.; Diabat, A. Integrated fuzzy multi criteria decision making method and multi-objective programming approach for supplier selection and order allocation in a green supply chain. *J. Clean. Prod.* **2013**, *47*, 355–367. [CrossRef]
78. Do, Q.H.; Chen, J.-F.; Hsieh, H.-N. Trapezoidal Fuzzy AHP and Fuzzy Comprehensive Evaluation Approaches for Evaluating Academic Library Service. *WSEAS Trans. Comput.* **2015**, *14*, 607–619.
79. Carter, H.; Dubois, D.; Prade, H. Fuzzy Sets and Systems—Theory and Applications. *J. Oper. Res. Soc.* **1982**, *33*, 198. [CrossRef]
80. Hsu, H.-M.; Chen, C.-T. Aggregation of fuzzy opinions under group decision making. *Fuzzy Sets Syst.* **1996**, *79*, 279–285. [CrossRef]
81. Xu, Z.S. A method based on the dynamic weighted geometric aggregation operator for dynamic hybrid multi-attribute group decision making. *Int. J. Uncertain. Fuzziness Knowl.-Based Syst.* **2009**, *17*, 15–33. [CrossRef]
82. Herrera, F.; Herrera-Viedma, E.; Verdegay, J. Direct approach processes in group decision making using linguistic OWA operators. *Fuzzy Sets Syst.* **1996**, *79*, 175–190. [CrossRef]
83. Kuo, M.-S.; Liang, G.-S. A novel hybrid decision-making model for selecting locations in a fuzzy environment. *Math. Comput. Model.* **2011**, *54*, 88–104. [CrossRef]
84. Mallick, S.K.; Rudra, S.; Maity, B. Land suitability assessment for urban built-up development of a city in the Eastern Himalayan foothills: A study towards urban sustainability. *Environ. Dev. Sustain.* **2022**, 1–26. [CrossRef]
85. Abdo, H.G. Assessment of landslide susceptibility zonation using frequency ratio and statistical index: A case study of Al-Fawar basin, Tartous, Syria. *Int. J. Environ. Sci. Technol.* **2021**, *19*, 2599–2618. [CrossRef]
86. Durante, P.; Martín-Alcón, S.; Gil-Tena, A.; Algeet, N.; Tomé, J.L.; Recuero, L.; Palacios-Orueta, A.; Oyonarte, C. Improving Aboveground Forest Biomass Maps: From High-Resolution to National Scale. *Remote Sens.* **2019**, *11*, 795. [CrossRef]
87. Wang, Y.; Hou, L.; Li, M.; Zheng, R. A Novel Fire Risk Assessment Approach for Large-Scale Commercial and High-Rise Buildings Based on Fuzzy Analytic Hierarchy Process (FAHP) and Coupling Revision. *Int. J. Environ. Res. Public Health* **2021**, *18*, 7187. [CrossRef]
88. Thungngern, J.; Wijitkosum, S.; Sriburi, T.; Sukhsri, C. A Review of the Analytical Hierarchy Process (AHP): An Approach to Water Resource Management in Thailand. *Appl. Environ. Res.* **2015**, *37*, 13–32. [CrossRef]
89. Wijitkosum, S.; Sriburi, T. Fuzzy AHP Integrated with GIS Analyses for Drought Risk Assessment: A Case Study from Upper Phetchaburi River Basin, Thailand. *Water* **2019**, *11*, 939. [CrossRef]
90. Abbas, H.; Khan, A.A.; Hussain, D.; Khan, G.; Hassan, S.N.U.; Kulsoom, I.; Hussain, S.; Bazai, S.U. Landslide Inventory and Landslide Susceptibility Mapping for China Pakistan Economic Corridor (CPEC)'s main route (Karakorum Highway). *J. Appl. Emerg. Sci.* **2021**, *11*, 18. [CrossRef]
91. Odion, D.C.; Hanson, C.T.; Baker, W.L.; DellaSala, D.A.; Williams, M.A. Areas of Agreement and Disagreement Regarding Ponderosa Pine and Mixed Conifer Forest Fire Regimes: A Dialogue with Stevens et al. *PLoS ONE* **2016**, *11*, e0154579. [CrossRef]
92. Abdi, O.; Kamkar, B.; Shirvani, Z.; da Silva, J.A.T.; Buchroithner, M.F. Spatial-statistical analysis of factors determining forest fires: A case study from Golestan, Northeast Iran. *Geomat. Nat. Hazards Risk* **2016**, *9*, 267–280. [CrossRef]
93. Bar, S.; Parida, B.R.; Pandey, A.C.; Kumar, N. Pixel-Based Long-Term (2001–2020) Estimations of Forest Fire Emissions over the Himalaya. *Remote Sens.* **2022**, *14*, 5302. [CrossRef]
94. Tomar, J.S.; Kranjčić, N.; Đurin, B.; Kanga, S.; Singh, S.K. Forest Fire Hazards Vulnerability and Risk Assessment in Sirmaur District Forest of Himachal Pradesh (India): A Geospatial Approach. *ISPRS Int. J. Geo-Inf.* **2021**, *10*, 447. [CrossRef]

Disclaimer/Publisher's Note: The statements, opinions and data contained in all publications are solely those of the individual author(s) and contributor(s) and not of MDPI and/or the editor(s). MDPI and/or the editor(s) disclaim responsibility for any injury to people or property resulting from any ideas, methods, instructions or products referred to in the content.